University of Genoa

Ph.D. program in Biotechnologies in translational medicine

Cellular responses to altered gravity: *in vitro* and *in vivo* insights into skeletal dynamics

Ph.D. student: Alessio Campioli

XXXVI cycle

Tutor: prof.ssa Sara Tavella

Ph.D. coordinator: prof. Paolo Malatesta

Abstract

Since the appearance of life on Earth, approximately 3.8 billion years ago, all organisms have been subjected to the continuous force of gravity, which has significantly influenced biological evolution and the development of organic structures. Gravity affects various tissues, particularly bone, which undergoes remodeling in response to changes in gravitational forces, such as those experienced in microgravity or hypergravity conditions. This study investigates the effects of altered gravity on bone tissue and the role of lipocalin-2 (LCN-2), a protein whose expression is influenced by microgravity condition.

In vitro experiments, were conducted using the MLO-Y4 murine osteocyte cell line to assess the impact of LCN-2 on bone metabolism. The addition of LCN-2 at a concentration of 200 ng/µL was found to increase the expression of peroxisome proliferator-activated receptor gamma (*Pparγ*), sclerostin (*Sost*), and osteocalcin (*Ocn*), podoplanin (*E11*) suggesting a role in bone cell differentiation and homeostasis. However, LCN-2 did not induce apoptosis in osteocytes, as indicated by the unchanged *Bax/Bcl2* ratio. Nevertheless, it did increase the expression of senescence-associated genes such as *P53*, *P21*, and *P16*, hinting at a potential role in osteocyte aging.

Additionally, the interaction between simulated microgravity, using the Random Positioning Machine, and LCN-2 presence was examined. Simulated microgravity in combination with LCN-2 revealed a synergistic effect on modulating the *Bax/Bcl2* ratio, while senescence genes were predominantly influenced by microgravity alone without a synergistic effect with LCN-2. Elevated levels of LCN-2 were detected in the serum of hindlimb unloading (HLU) mice, which simulates microgravity conditions in rodents. A higher concentration of LCN-2 (1000 ng/µL) was then tested, revealing similar impacts on the *E11* gene, associated with bone homeostasis, but not on genes related to bone cell differentiation. The influence on apoptosis and senescence was observed, although the changes were not statistically significant, with the exception of *P53*. More investigations are needed to elucidate the complex role of LCN-2 in bone homeostasis.

The in vivo segment of the study assessed the effects of hypergravity through a 14-day preliminary experiment followed by a 27-day extended investigation. Health indicators such as water intake and body weight were monitored, along with gene expression in the femurs and tibiae of the mice.

Results suggested that a sustained exposure to hypergravity (3g) for 27 days prompted a shift towards bone deposition, as evidenced by the expression of bone formation markers *Col1a1* and *Ocn* and remodeling markers *Rankl* and *Opg*. These findings were supported by MicroCT scans showing increased bone volume and cortical thickness in hypergravity-exposed mice compared to controls. Inversely to the effects seen in simulated microgravity, LCN-2 expression was downregulated by hypergravity, underscoring its potential role in the body's response to changes in gravitational forces.

CONTENTS

1.0 INTRODUCTION

Space exploration represents an important milestone and an exciting endeavor in the evolution of human species. This advancement would provide the opportunity to access valuable resources and new spaces, allowing the long-term survival of humanity.

However, great achievements do not come without difficulties. Space and lands (Moon and Mars) that we aim to reach in the near future, present indeed extremely inhospitable environments for life, characterized by conditions vastly different from those familiar on Earth. Main complications may be related to the lack of a robust magnetosphere, protecting from cosmic rays, as well as the low gravitational forces on celestial bodies. Additionally, the absence of gravity during interplanetary travel, known as microgravity presents further complications.

Specifically, this project will be focused on studying the effects of altered gravity *in vitro* and *in vivo* into skeletal dynamics. To this extent, some fundamental notions will be introduced in the following paragraphs.

1.1 BONE

Bone is a tissue composed of different types of cells, each with its specific role. Bone is a specialized connective tissue hardened by mineralization with calcium phosphate in the form of hydroxyapatite ($[Ca_3(PO_4)_2]Ca(OH)_2$). At the tissue level, we must imagine the bone as a system continuously remodeled by resorption and formation processes. If resorption is favored we will have greater osteoclastic activity which will lead to loss of bone mass. Many diseases are linked to this imbalance, creating a systemic or local bone loss. Bone has an intrinsic ability to adapt its morphology by adding new bone to withstand increased amounts of loading, and by removing bone in response to unloading or disuse. [1–3]

The transformation of mechanical stress into biochemical signals occurs in osteocytes and osteoblasts and involves a variety of membrane proteins, including integrins, connexins and stretch-activated ion channels. Mechanical stimulation increases expression of connexins, membrane-spanning proteins that form regulated channels; this allows the direct exchange of small molecules with adjacent cells, resulting in intercellular communication between cells. It has been shown that mechanical stimulation increases expression of connexins. Connexins can also form regulatory hemi-channels between the cell and its extracellular environment. Shear stress leads to the

modulation of release of nitric oxide and eicosanoid from osteoblasts and osteocytes, which may be due to activation of nitric oxide synthase. For these reasons, mechanical strain is a key regulator of osteoblast and osteoclast activity, these two cells will be described below[1,3].

Osteoclasts are end-differentiated multinucleated cells of monocyte/macrophage lineage that are formed to carry out the unique function of resorbing bone matrix. Subsequent investigations have shown that osteoclastogenesis is critically dependent on two key cytokines, namely RANKL (receptor activator of nuclear factor-kB ligand), also known as TRANCE (TNF-related activation-inducing cytokine) and M-CSF (monocyte-colony stimulation factor). Osteoclasts create a lysosomal compartment (ruffled border) where the acidic pH (around 4) solubilizes the mineral component while the proteolytic enzymes digest the matrix[4].

On the opposite side, protagonists of bone construction, we have osteoblasts, cells capable of secreting matrix proteins. Among the proteins of the extracellular matrix, we have type I collagen which constitutes 90% of the matrix but also non-collagenous proteins such as osteopontin, osteonectin, and bone sialoprotein. They also possess high levels of Alkaline Phosphatase (ALP), a fundamental protein in mineralization processes. These cells work closely together to produce the lamellar structure characteristic of bone. Unlike osteoclasts, they originate from stem mesenchymal cells. A part of the osteoblasts is lodged inside the bone becoming osteocytes while others flatten themselves on the surface of the bone becoming lining cells. The process of osteocyte differentiation, whereby osteoblasts become encased in mineralized bone matrix is not yet fully understood. The most abundant matrix protein in the osteocyte environment is type-I collagen. Osteocyte phenotype and the formation of osteocyte processes has been shown to be dependent on cleavage of type-I collagen[1,2,4].

Osteocytes, cells that also participate in bone turnover, residing in lacunae distributed within the matrix communicate through their interconnecting dendritic processes through a large lacuno-canalicular network which allows osteocyte communication with cells on the bone surface and access to the nutrients in the vasculature. Osteocytes make up approximately 90-95% of all bone cells and are the cells with the longest lifespan, living up to a decade together in their mineralized environment. Osteocytes produce a range of signal molecules capable of regulating osteoblastogenesis such as prostaglandin E2, growth factors (activation) or sclerostin (inhibition). Furthermore, osteocytes secrete receptor activators of nuclear factor B ligand (RANKL) which

induces osteoclastogenesis. Furthermore, osteocytes are able to regulate phosphate metabolism and biomineralization through molecules such as PHEX, DMP-1, MEPE and FGF-23. DMP-1 and PHEX appear to downregulate the expression of FGF-23 which is in turn linked to phosphate reabsorption in the kidneys. The osteocytes can sense the mechanical loads and coordinate adaptive alterations in bone mass and architecture but is not yet completely understood. It is accepted that mechanical loads placed on bones generate several stimuli like physical deformation of the bone matrix itself load-induced flow of canalicular fluid through the lacuno-canalicular network and electrical streaming potentials generated from ionic fluid flowing past the charged surfaces of the lacuno-canalicular channels[3,4].

The two main structural types of bone are cortical and cancellous bone. Although both have the same overall matrix composition, they differ significantly in three important ways: density or porosity, three-dimensional structure, and metabolic activity. These three factors influence their function and physiology to a great extent. The two main structural types of bone are:

The cortical bone, the outermost part of most bones, is responsible for supporting function. Osteons form the major structural unit of cortical bone and the bulk of the diaphysis. They consist of longitudinal cylinders that run in parallel to the long axis of the bone. Osteons are formed from concentric lamellae surrounding central Haversian canals, which are lined by endosteal cells and contain blood vessels, lymphatics, and occasionally nerves. Cell processes, or canaliculi, from osteocytes extend in a radial pattern from the central canal like spokes of a wheel. These canaliculi connect the central canal to osteocytes, allowing diffusion of nutrients through the bone matrix.

The trabecular bone (or Cancellous), the innermost part which is much more metabolically active. Trabecular bone is a highly porous, heterogeneous, and anisotropic material which can be found at the epiphyses of long bones and in the vertebral bodies. Trabecular bone is the main load bearing bone in vertebral bodies and also transfers the load from joints to the compact bone of the cortex of long bones. At a microstructural scale, trabecular architecture is organized to optimize load transfer. Mineral and collagen content and architecture determine the mechanical properties of trabecular bone tissue. Cancellous bone also contains lamellar bone, albeit with a different structure than the osteon. Cancellous lamellae are arranged in semicircular shapes called “packets,” which three dimensionally form the visible bony trabeculae[5,6].

The bone, as already mentioned, can perceive mechanical stresses mainly linked to the force of gravity, for this reason, some notions will be introduced, and discussed in the next chapters.

1.2 GRAVITY

Gravity is one of the four fundamental forces governing the universe and we experience it every day in our life. It was first defined by Isaac Newton in 1687, in the book *Philosophiae Naturalis Principia Mathematica* where he elegantly formulated it with the equation showed in figure 1.

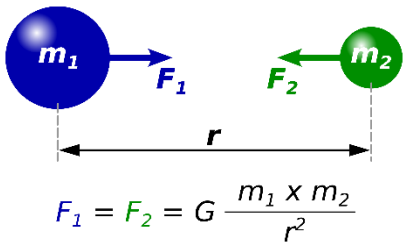

FIG. 1 EQUATION OF UNIVERSAL GRAVITATION [7]

The intensity of the force is related to the masses of the objects involved and inversely proportional to the square of the distance between them. However, Newton never explained this phenomenon and it took nearly 200 more years for a young Albert Einstein to provide a more profound explanation. Einstein redefined gravity as an apparent force resulting from the curvature of space-time caused by the presence of mass and energy. This revolutionary insight fundamentally changed our understanding of gravity and the nature of the cosmos.

1.3 MICROGRAVITY

Microgravity is the condition in which objects appear to be weightless. If we were aboard the International Space Station (ISS), we might expect to feel the force of the gravity. However, apparently this does not happen, because we would actually be in a state of perpetual free fall. The ISS is indeed continuously attracted towards the center of the Earth, but its high orbital velocity theoretically prevents it from falling. However, this is not entirely accurate due to the slowing down of its speed caused by a slight friction depending on the extremely rarefied but still present atmosphere. The peculiarity of this state is the possibility to simulate a condition that would be challenging to recreate on Earth.

This condition is extensively studied on materials, on organisms *in vitro* and *in vivo* but it is experienced also by astronauts living inside the ISS [8]. Long-term residence in space may indeed have

adverse effects on biological organisms. In this scenario, some missions demonstrated the consequences of extended permanence in space, such as the Scott Kelly's one, who conducted the "One Year Mission" by spending a year in orbit on the ISS [9].

Different studies highlighted two main problems related to the life in space, from the biological point of view:

1. High Levels of Radiation: Radiation exposure in space, whether on the ISS, during interplanetary travel to Mars, or during prolonged stays on celestial bodies, is significantly higher than the background radiation levels on Earth. This phenomenon causes many issues for the human body, including weakening of the immune system and increased probability of cancer development. Furthermore, this radiation can become particularly hazardous and potentially fatal in case of rare events, such as solar flares.
2. Microgravity or reduced gravity: the lack of adequate gravity could affect human organism homeostasis. Various organs can be interested, but musculo-skeletal system is particularly sensitive to mechanical loading alterations. Since there is no continuous gravitational stimulus as experienced on Earth, tissues undergo remodeling, and their homeostasis can be impaired, making rehabilitation periods necessary.

For these reasons, further studies are needed to elucidate the effects of microgravity on the skeletal system. Despite the great interest on this topic, highs costs and difficulties related to transport of the experiment into Earth orbit, and specifically on the ISS, still represent a limit. In this scenario, it was essential to create alternative systems for simulating microgravity condition. Historically, the first instrument used to simulate the absence of gravity was the clinostat, invented by Julius von Sachs in 1879 (Fig. 2 and 3). This tool was adopted to eliminate the effect of gravity on plants, but it was not suitable for other organisms, since they are influenced by rapid changes in orientation over short periods. Another constraint of this apparatus is that it only allows rotation along a single plane and does not provide movement in three dimensions.

FIG. 2 JULIUS VON SACHS [10]

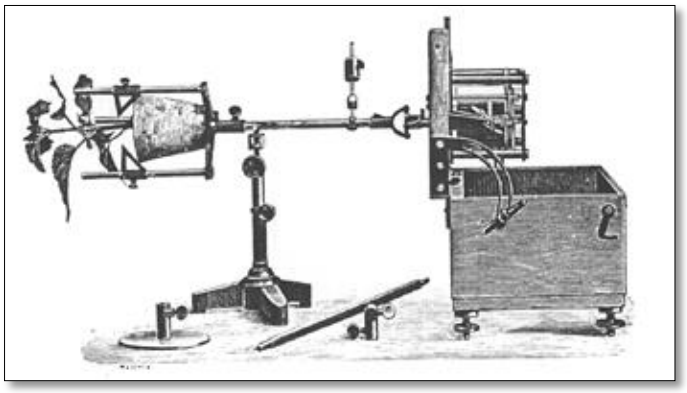

FIG. 3 CLINOSTAT [11]

Later, 3D clinostat was introduced and an improved version, called Random Positioning Machine (Fig.4), was developed. This advanced tool proved to be more effective in simulating microgravity conditions because it incorporates randomized changes in both the speed and direction of rotation over time.

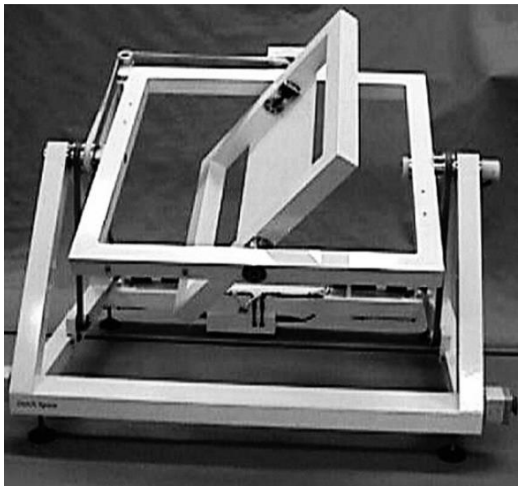

FIG. 4 RANDOM POSITIONING MACHINE (RPM) [12]

The random movement at low speeds to make the centrifugal force minimal occurs in the three dimensions, allowing to obtain an average gravity vector equal to zero and therefore to simulate

extremely low gravity values. Due to the movement of the instrument, it is advisable that the experiment need to be positioned in the center in such a way as to minimize the effect of centrifugal force.

A parallel version of the previous instrument is represented by Rotating Wall Vessel, in which the cells are bound to spheres immersed in the culture medium in a rotating cylinder. By adjusting the rotational speed, it is possible to bring the spheres into a simulated free fall situation. Precise control of the speed is crucial, since a too low speed would lead the cells to settle while too high speed would lead them to adhere to the surface of the cylinder, simulating an apparent gravitational force associated with the centrifugal force (Fig. 5).

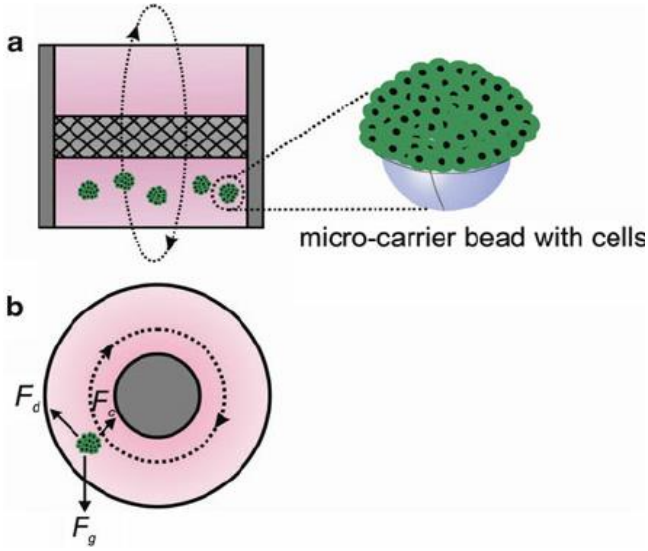

FIG. 5 ROTATING WALL VESSEL [13]

1.3.1 EFFECT OF MICROGRAVITY ON MUSCULO-SKELETAL SYSTEM

Extended human spaceflight was once a distant fantasy. However, it is now on the verge of becoming a tangible reality, making the understanding about impacts of long-term space travel on human health more critical than ever[14]. As introduced before, the loss of gravitational force is a major prohibitive environmental factor that adversely affects the body of space travelers. The human body is intrinsically adapted to Earth's gravity and exposure to microgravity can lead to complications in normal physiological functions. Data gathered from astronauts, coupled with animal and cellular experiments conducted in space, unequivocally revealed that microgravity

induces skeletal deconditioning in weight-bearing bones. Consequently, this leads to a significant reduction in bone mass, which increase the risk of fractures and osteoporosis[15]. Furthermore in microgravity, the unloading of musculoskeletal tissues occurs, leading to muscle atrophy and a shift in muscle fiber properties.

This knowledge is essential for mitigating the health challenges associated with extended missions beyond Earth.

Before delving into how microgravity affects bone health, it is important to understand bone function in normal gravity conditions. Under normal circumstances, bone remodeling is an adaptive and balanced process where bone resorption and formation are coupled to regulate homeostasis of bone tissue [16]. The overall process relies on osteoblasts and osteoclasts acting in concert to regulate bone formation and resorption, respectively.

The weightlessness experienced in microgravity reduces the loading on weight-bearing bones, resulting in adaptive changes that increase bone resorption and inhibit bone formation [17]. Several mechanisms have been proposed to explain this bone homeostasis impairment.

Osteocytes were described to have a role in microgravity-related bone loss. Osteocytes normally reside in lacunae of the mineralized bone, where they synthetize proteins such as collagens, which will be part of the bone matrix itself [18]. They were reported to undergo apoptosis after microgravity exposure, leaving consequently an increased number of empty lacunae, or lacunae with reduced volume and altered shape. This may trigger further bone resorption, leading to the deterioration of bone microstructure and loss of bone mass [19].

Mechanical stimulation has been demonstrated in the literature to be important in the cellular survival mechanisms of osteocytes *in vitro* [20]. These data were also confirmed in *in vivo* experiments (on mice) where the reduced application of mechanical force led to an increase in osteocyte apoptosis [20].

The effect of the lack of mechanical loading has also been seen in simulated microgravity models on humans such as the bed rest. The Bed rest is a model where healthy subjects are confined to the horizontal or head-down tilt position (HDT) for extended periods. This is a recognized experimental

analog to induce some of the physiological adaptations experienced by astronauts during spaceflight[21].

Osteocytes are able to perceive the effects of the alteration of gravity through important mechanosensors, therefore they can be affected by the presence or absence of gravity and these sensors could transmit information to the cell. The importance of such sensors is also demonstrated in the literature, reporting that the lack of CX43 (mechanosensor protein) in osteocytes leads to greater apoptosis but also to protection from further bone loss in simulated microgravity[22]. In turn, osteocytes can transmit information through signal molecules to the two main effector cells, namely osteoblasts and osteoclasts.

In this regard, some signal molecules, produced by osteocytes, have been identified which would have a direct role in influencing the activity of affected cells, osteoblasts and osteoclasts.

Among these, Sclerostin is a *SOST* gene product that reduces osteoblastic bone formation by inhibiting canonical Wnt/β-catenin signaling[23]. It is a signal molecule that has been seen to increase in astronauts [24] but also in simulated microgravity models in humans, such as stimulation for 90 days in bed rest [25]. Moreover, RANKL is a type II transmembrane protein found on the surface of cells as a proteolytically released soluble form [26]. Osteoclast differentiation predominantly depends on RANKL signaling (encoded by *TNFSF11* gene) [27]. RANKL was initially identified as being produced by osteocytes, but recent findings report that *RANKL* is expressed by a wide variety of cells including osteoblasts, osteocytes, and bone marrow adipocytes and it is still unclear which of these sources activate osteoclast formation[28].

One of the most reported observations is related to changes in osteoblast cell morphology, which is reflected in active cytoskeleton collapse after microgravity exposure [29,30]. Furthermore, most of the current literature consistently reports that simulated microgravity inhibits the proliferation and differentiation of mesenchymal stromal cells (MSCs) towards osteoblasts[31]. Osteoclasts also can contribute to space-related bone loss by disrupting normal bone homeostasis. They indeed exhibited an increased resorptive activity in response to microgravity compared to controls on Earth [32 33].

Finally, studies on the reduction of bone mass have shown that there is a correlation between bone loss and apoptosis, and in recent times also the senescence of bone cells. An increase in apoptosis

was observed in rodent animal models in both real[19] and simulated microgravity (HLU)[34]. *In vitro* studies reported that osteocytes exposed to simulated microgravity showed an increase in apoptosis markers, BAX and BAD. On the other side, senescence is one of the main causes of bone loss in aging-related osteoporosis. The effect of microgravity in inducing bone senescence is not well documented in the literature. Blaber et all documents bone loss in mice after exposure to real microgravity for 15 days caused by osteoclastic activity, osteocytic osteolysis and increased expression of *P21* in osteoblasts. P21 is an important marker of senescence that inhibits the cell cycle, Blaber claims that there could be a correlation between the stop of the cell cycle during osteogenesis contributing to bone loss in space[35].

1.4 HYPERGRAVITY

Since life first set foot on this planet, gravity has always been present, shaping the organisms influenced by it. It is reasonable to assume that most organisms have evolved sensors and structures tailored to this force. But what happens if a greater force is applied? Which is the body's response?

Hypergravity is defined as the condition in which the force applied to an object or organism exceeds the standard terrestrial value (i.e., 1 g). Under normal circumstances, we experience relatively consistent gravitational forces, with slight variations primarily dependent on our distance from the Earth’s center. For example, if we refer to Genoa, the gravitational acceleration will be approximately 1g (because we are at sea level). On Mount Everest it is equal to 0.9967 g, while on the ISS, which orbits 400 km above Earth, it is 0.89 g. It is reasonable to assume that there are no significant effects on the human body mainly related to variations in gravitational force.

The study of hypergravity began in 1806 with a series of experiments on the effects of artificial gravity on plants, aiming at understanding how a centrifugal force could influence the direction of plant growth[36].

In the present day on Earth, hypergravity can be simulated through rotating systems, and one notable example is the ESA's Large Diameter Centrifuge. By placing an object or an organism on a platform attached on the centrifuge, the force experienced by the object is directly proportional to the centrifuge's rotational speed. This is the easiest way to generate a velocity-controlled g-force. These simulation systems have also been used on humans for years. Astronauts and jet pilots are indeed placed on custom-made centrifuges to test their ability to withstand high g values. This helps

prepare their bodies for sudden changes in acceleration, which they may experience during rocket launches or re-entry into the atmosphere.

Since data on both microgravity and hypergravity suggest that their effects could potentially offset one another, the idea of building a centrifuge to create artificial gravity in space gained ground[37]. This concept suggests that rotating space stations, similar to those proposed by Von Braun (Fig.6) or imagined by Kubrick in the film "2001: A Space Odyssey" (Fig.7) could become a reality. There are currently no projects underway with the aim of creating structures of this type, such constructions still represent a great engineering challenge and the cost is also prohibitive.

Such space stations could help astronauts to counterbalance the detrimental effects of microgravity and make long-duration space missions more feasible.

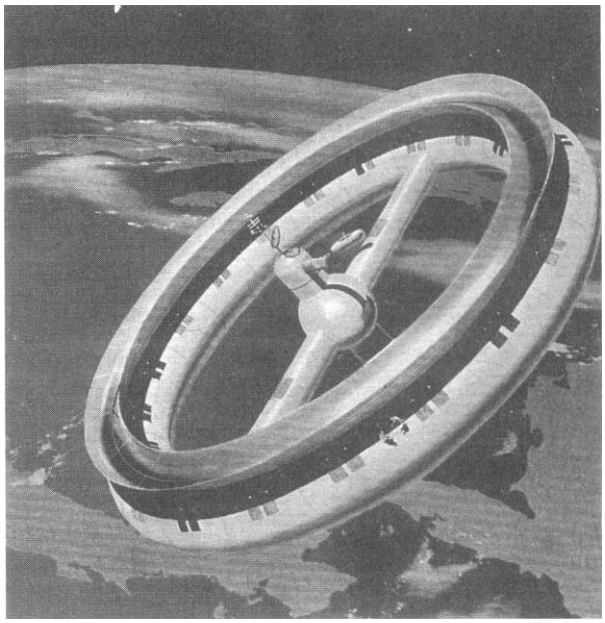

FIG. 6 VON BRAUN'S ROTATING SPACE STATION[37]

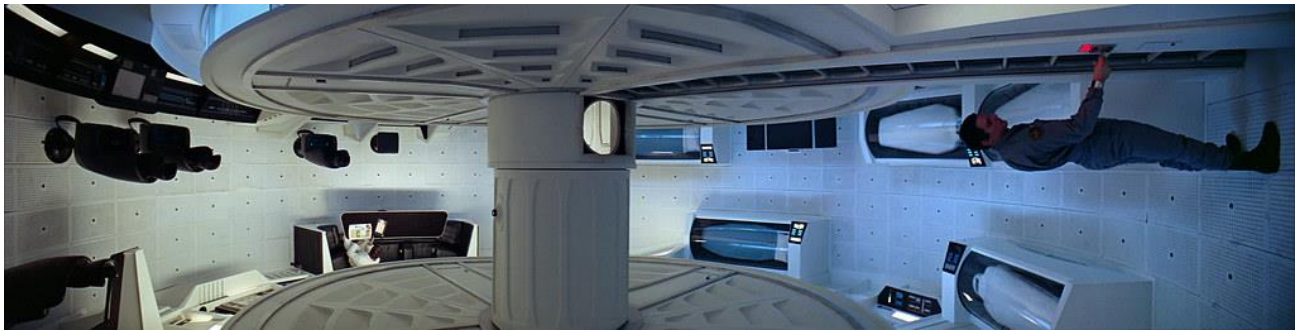

FIG. 7 FRAME FROM KUBRICK FILM, 2001: A SPACE ODYSSEY

1.4.1 EFFECTS OF HYPERGRAVITY ON MUSCULO-SKELETAL SYSTEM

It is well known that skeletal muscle undergoes adaptive changes in terms of both fiber size and contractile phenotype in response to variations in loading conditions[38]. Microgravity and hypergravity have contrasting effects on musculoskeletal tissues. In microgravity, as mentioned earlier, the unloading of musculoskeletal tissues occurs, leading to muscle atrophy and bone loss. In contrast, hypergravity, which represents conditions of increased gravitational force, appears to counterbalance the negative effects of microgravity on musculoskeletal tissues. However, hypergravity effects on the musculoskeletal system are not widely studied, and its potential side effects remain largely unexplored. Understanding the impact of both microgravity and hypergravity on muscle and bone health is essential for developing strategies to maintain astronaut well-being during space missions. For instance, studies involving mice in different gravitational conditions have provided valuable insights. Hypergravity can cause an alteration in cell viscosity, which suggests an adaptation of the cells to changes in g-force through presumably a restructuring of the cytoskeleton[39]. Additionally, research by Kawao and colleagues in 2016 demonstrated that vestibular signals, which are related to balance and spatial orientation, can also induce changes in the musculoskeletal system under hypergravity conditions [40]. This underscores the significant role of the nervous system in mediating bone remodelling processes, further emphasizing the complexity of the body's adaptation to different gravitational environments. As already mentioned, bones have important mechanical sensors capable of perceiving gravity and are also able to adapt to these changes in mechanical load. In this regard it is important to mention Wolff's rule. This statement describes the effect of mechanical loading and how the bone responds to it [41]. This effect is widely demonstrated in microgravity as previously reported. While, with regards to hypergravity, this rule is confirmed for example by Vico et all where increased bone mass was seen, especially Cancellous bone in tibial metaphysis, of rats after centrifugation in 2 g for 4 days[42]. In microgravity, when exposed to 1 g artificial gravity, mice showed a reduction in bone mass, while in a ground-based experiment where mice were exposed to 2 g there was even an increase in bone volume compared to control [43]. In our previous work, it was demonstrated that exposure to hypergravity (2g) for 90 days brought about structural changes to the bone, hypergravity condition induces thickening of the cortical bone and a higher percentage of large-sized trabecular in the Cancellous bone[44].

1.5 LARGE DIAMETER CENTRIFUGE (LDC)

The Large Diameter Centrifuge (LDC) is a centrifuge facility located at the European Space Research and Technology Centre (ESTEC) in Noordwijk and developed by the European Space Agency (ESA) (Fig.8). It has an impressive diameter of 8 meters, with 4 arms to which a maximum of 6 gondolas can be connected. Each gondola can support a maximum load of 80 kg and is equipped with an electrical network (230 volts), interfaces for data transmission (USB, Ethernet and video connection), and connections for the transport of air, gas or water, essentials for conducting long-term experiments. To ensure the proper monitoring of the experiment, each gondola has temperature and acceleration sensors, which help track environmental conditions and the forces experienced during centrifugation. Additionally a seventh gondola can be added in the center of the centrifuge as a reference control. Although it is also affected by the rotation, it experiences a constant gravitational force (g=1) and serves as a reference for experiments conducted on the other gondolas subjected to varying levels of artificial gravity due to the centrifuge's rotation.

FIG. 8 LARGE DIAMETER CENTRIFUGE (LDC)[45].

The artificial gravity generated by this instrument follows the Coriolis type (like in rotating wall vessel), which is characteristic of rotating systems. Being a gravity created by a rotating system means that this is not a pure g force like the one we experience every day. The Coriolis Effect associated with rotation becomes more pronounced with rapid changes in angular acceleration. This

is why the start of the experiment requires a slow achievement of the speed (suitable for simulating artificial gravity) and the use of a reliable system to maintain a constant speed throughout the experiment. From studies involving humans, it's been observed that the Coriolis force not only leads to visual disorientation but also adversely affects motion sensation from the inner ear structures, causing imbalance and dizziness[46]. One noteworthy detail is that two systems with different radius but with the same number of revolutions per minute will produce the same Coriolis force, and for this reason, the LDC was built with a diameter of 8 meters. The value of g generated inside the gondola is proportional to the following equation:

$$a_c = \omega^2 r$$

Where a_c is the centripetal acceleration, ω is the angular velocity while r is the radius which in this case is 4 meters. So the centripetal force on the gondola will be:

$$F_c = ma_c = m\omega^2 r$$

Having also the force of gravity as a force applied to the gondola, the acceleration force experienced inside the gondola will be the resultant of the gravitational acceleration vector and the centripetal acceleration vector:

$$a_{exp} = a_c \cos(\alpha)$$

Where α is the angle of inclination of the gondola with respect to the rotating arm. Furthermore, as already mentioned, there is a contaminant in this g-force generated, related to the Coriolis force[47] . Our research group was involved in two different experiments, placed in 2019 and 2023, respectively, aiming at exploring the effect of altered gravity on mice. In both experiments, the LDC was used to simulate a force of 3 g on mice, which were placed within the Mice Drawer System, a module previously used in 2009, for experiments in microgravity (STS-128; STS-129[48,49]) .

1.6 MICE DRAWER SYSTEM (MDS)

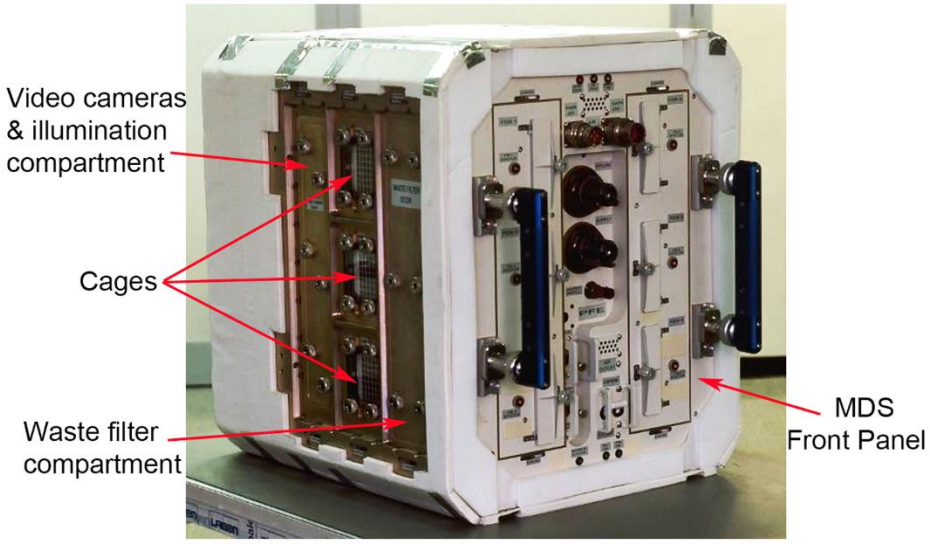

FIG. 9 MICE DRAWER SYSTEM (MDS) [50]

The Mice Drawer System is a module of the Italian Space Agency (ASI) designed in 1998 by Thales Alenia Space – Italy, created specifically to be transported into space (missions STS-128, STS-129) and to carry out microgravity experiments on small animals like rodents (mice and rats)[50]. Each module has different components, the Mice Chamber (MC), the liquid handling subsystem (LHS), the food delivery subsystem (FDS), the air conditioning subsystem (ACS), the illumination subsystem (ILS), the observation subsystem (OSS) and the payload control unit (PCU). Each module has also 6 cages, each cage can host a mouse and has dimensions of 116 x 98 x 85 cm. Furthermore, each cage contains food bars, valves for water delivery, a camera, white and infrared LEDs (for night vision) and temperature, humidity and air quality (CO_2 and NH_3) sensors. More specifically, the Liquid Handling Subsystem allows the transport of water to the 6 cages and is connected to the 0.5 L main water tank. The food Delivery system provides the mice with 2 bars of food per cage, quantity and administration period can be programmed for each individual cage. The air conditioning subsystem (ACS) maintain a flow of fresh, clean air, which mixing with the internal air removes the produced CO_2, by replenishing oxygen levels. This is accomplished by exchanging approximately 5% of the air within the space with fresh outside air every 2 minutes. Furthermore, to prevent microbiological contamination, the system incorporates HEPA filters at both the inlet and outlet. Initially, this design was put in place to safeguard the mice from potential infections originating from the external environment, but also to prevent the mice themselves from releasing bad smell and pathogens into the air that the astronauts breathed. In addition, ACS has the function of removing waste products

such as urine, feces, hairs and other debris through the waste filters which are positioned under each cage and must be changed every 30 days. ACS can finally maintain the temperature between 25 and 30 degrees and passively control humidity (through a desiccant in the waste filters).

The illumination subsystem allows the creation of the day/night cycle fundamental to the animal's circadian rhythm. During the day, this system provides diffused lighting through white LEDs, while at night, it can be switched to infrared LEDs to allow for night time observation. The total brightness is maintained at 40 LUX with the flexibility to make small 2 LUX variations to simulate the transition from day to night and vice versa.

The observation subsystem enables continuous monitoring of the animals through a camera both during the day and at night. This ensures that their behavior and activities can be observed and recorded throughout the experiment.

Finally, the payload control unit not only provides autonomy to the MDS module but also allows for the execution of external commands and monitoring of the module's condition. Furthermore, all the information and commands can be stored within the MDS internal memory[50].

This advanced cage system was used for the Tissue Sharing Program (TSP) experiments conducted in 2019 and 2023. The TSP involves various research groups from different parts of the world, including Italy, Japan, United States, Belgium, Netherlands, United Kingdom, France and Germany, with their specializations as protagonists (Fig.10).

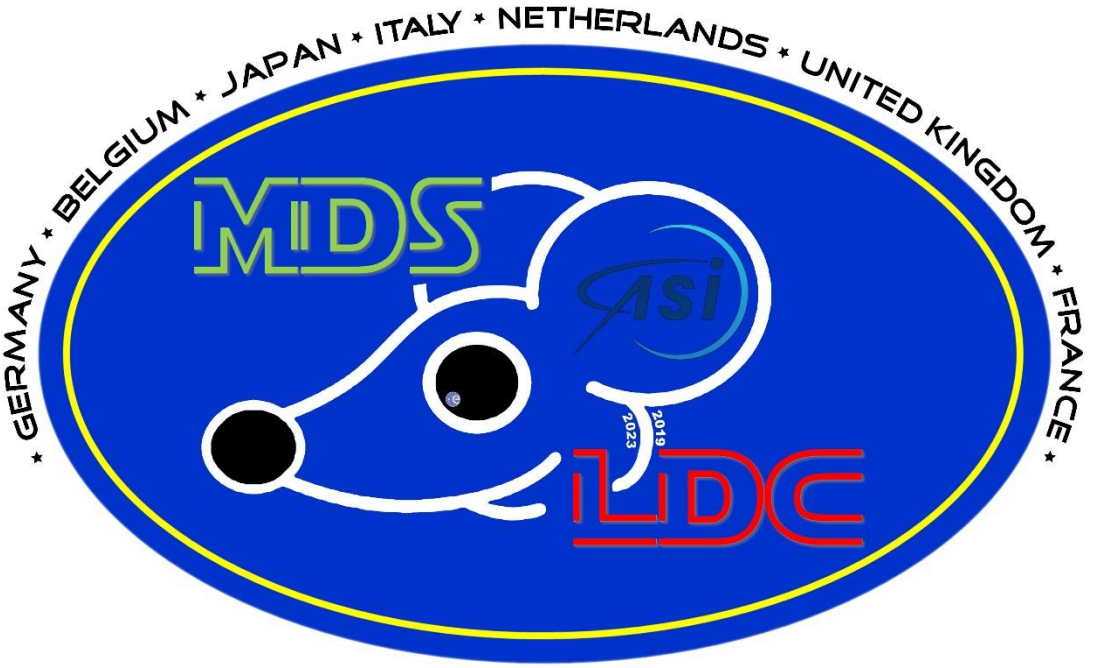

FIG. 10 TISSUE SHARING PROGRAM MISSION LOGO

1.7 LIPOCALIN-2

Lipocalins are a large multifunctional family of small proteins (15-25kDa) first discovered in eukaryotes and then also discovered in bacteria[51]. These proteins have a structure containing a cavity that makes them capable of carrying small hydrophobic molecules. According to some studies, these proteins are overexpressed under stressful conditions [52] [53].

Specifically, Lipocalin-2 (LCN-2) also known as Neutrophil Gelatinase-Associated Lipocalin (NGAL), is an adipokine with a variety of functions in different organs. LCN-2 overexpression is associated to various processes of inflammation, tissue remodeling, chronic kidney disease, energy metabolism, tumor development and progression. Furthermore, its presence is also related to bone metabolism processes connected to mechanical stimulation [54] .

The overexpression of LCN-2 has been observed in different simulated microgravity models (bed rest, cell cultures in RPM) and in our laboratory we have shown that its overexpression induces osteopenia in a transgenic mouse model [55]. For these reasons it has been proposed that lipocalin-2 is a stress protein involved in organs and tissues modifications induced also by the absence of gravity. According to this, we investigated if a high value of g experienced by a mouse, could alter the LCN-2 expression.

The combination of spaceflight and simulation data on humans, animals and cellular models will allow to improve the knowledge on microgravity induced bone loss. The use of cellular models has shed light into the molecular mechanisms behind this process. Interestingly, transcriptome studies on models of simulated microgravity showed that the most up regulated gene compared to unit gravity condition was the adipokine Lipocalin-2 (LCN-2), whose function in bone metabolism is poorly known [56].

1.8 AIM OF THE PROJECT

In this research, we aim to investigate the impact of altered gravity on skeletal tissue and bone cells, with a specific focus on the effects of Lipocalin 2. Our approach involved cell culture experiments under simulated microgravity exposure using RPM, animal models in HLU, and studies in hypergravity with an animal model at the Large Diameter Centrifuge in Noordwijk (NL) under 3g conditions.

2.0 MATERIALS AND METHODS

2.1 MATERIALS & REAGENTS

MEM alpha (Minimum Essential Medium alpha) and fetal bovine serum (FBS) are produced by Gibco, penicillin-streptomycin solution and trypsin are from Euroclone while L-glutamine is supplied by Sigma-Aldrich. LCN-2 (recombinant mouse) is produced by R&D systems while the plastic material used for cell cultures comes from SARSTEDT and FALCON. The Qiazol and the reverse transcription kit is from Qiagen, the primers from TIB MOLBIOL and Merck and the Takyon™ Low ROX SYBR 2X MasterMix from Eurogentec. The ELISA kits are produced by R&D systems.

2.2 CELL LINES

2.2.1 MLO-Y4

MLO-Y4 cell line is an osteocyte cell line derived from *Mus musculus* and purchased by Kerafast at passage 33. MLO-Y4 is derived from a transgenic mouse in which the immortalizing T-antigen was expressed under control of the osteocalcin promoter. These cells express considerable levels of E11 that appears to play a role in dendrite formation, an essential process for osteocytes to generate their network[57] . MLO-Y4 were cultured in α-MEM (GiBCo, Waltham, MA, USA), supplemented with 10% FBS (GiBCo) and 100 U/ml Penicillin/100 mg/ml Streptomycin (Euroclone, Milan, Italy), on 0.01% collagen (type I from rat tail) coated dishes (Sigma-Aldrich). Cells were maintained in a humified incubator, at 37°C, with 5% CO_2 and medium was changed every two days. Cells were expanded until passage 36, then used for further experiments, as described below.

2.3 HINDLIMB UNLOADING MODEL

Hind limb Unloading Model (HLU) is a model used for the first time in the mid-1970s by NASA and then spreaded to various laboratories around the world. It was adopted to simulate weightlessness and therefore microgravity. In this model, the hindlimbs of rodents are elevated to produce a 30° head-down tilt, which results in a cephalad fluid shift and avoids weightbearing by the hindquarters. This model has proven to be very useful for studying the physiological responses and unloading processes of mice but also the recovery processes (including tissue reloading) of mice [58].

This test was performed in collaboration with the group of prof. Maria Grano, in University of Bari, where mice were exposed in HLU for 4 weeks. Effects were analyzed through both RNA extraction from bone and subsequent Real Time PCR, and ELISA immunoassay on serum, against LCN-2.

2.4 RANDOM POSITIONING MACHINE

The Random positioning machine (RPM, Dutch Space) has been used to simulate the microgravity environment. It is connected to movements controlling unit and to a PC. The software allows to set different types of movements, for microgravity simulation. A “Random Mode” set up, in which the plane rotates on two different axes, randomly changing the direction at a speed between 30°/s and 60°/s, was used in this study.

RPM is hosted in a temperature-controlled room (37°C). Therefore, all the cells that are incubated onto RPM need to buffer the MEM alpha medium with HEPES (25 mM), $NaHCO_3$ (700 mg/L) and NaCl (300 mg/L) to maintain pH constant.

2.5 LCN-2 TREATMENT

MLO-Y4 cells were treated with LCN-2 in three independent experiments. In each experiment cells were seeded at a density of 5.000 cells/cm^2 and after 48 h the medium was changed. First experiment was carried out by leaving cells in culture for further 5 days and then treating them with 200 ng/mL LCN-2 in the last 8 h of experiment. In a parallel experiment, cells were cultured for further 2 days and then treated with 1000 ng/mL LCN-2 for 48 h hours. After treatments, cells were collected in Qiazol and stored at -80°C for RNA extraction and gene expression analysis.

In a third experiment, MLO-Y4 cells were cultured for 5 days and then treated with 200 ng/ml LCN-2 for the last 8 h of experiment or left in standard culture medium as control. The experiment was performed in RPM machine, for microgravity simulation. A control in standard culture medium was also carried out, by culturing the cells in a normal incubator in parallel (ground control).

2.6 SEAHORSE ANALYSIS

For this experiments, 10^5 MLO-Y4/well were seeded in XFp cell plates and centrifuged gently with no brake at 40 g for 3 min; after the stop the plate was then rotated 180° before centrifugation again at 80 g for 3 min to encourage adhesion to the plate and the forming of an evenly dispersed monolayer. Oxygen consumption rate (OCR) were determined using the Seahorse XFp Extracellular Flux Analyzer (Agilent Technologies, Santa Clara, CA, USA). Cells were then incubated at 37 °C for 45 min in a CO2-free incubator with Agilent Seahorse DMEM, pH 7.4, enriched with glucose (11 mM). OCR was monitored according to the manufacturer’s instructions. Briefly, three measurements of OCR was taken under control conditions, after the injection of 1.5 µM oligomycin (ATP synthase

inhibitor) and, thereafter, of 0.5 µM rotenone and 0.5 µM antimycin A to inhibit Complex I and III, respectively.

2.7 WESTERN BLOT

Total proteins were extracted from untreated and treated MLO-Y4 cells using 100 ul RIPA buffer (Thermo Fisher). Cells were kept on the ice for 30 min, each 5 min vortex for 30 sec. After 30 min, they were centrifuged for 20 min at max rpm at 4°C to pellet the cell debris. The supernatant containing the total soluble proteins was quantified by the Qubit Protein Assay kit (Thermo Fisher). Equal amounts of protein were loaded into each well of SDS-polyacrylamide gels (12%). Proteins were then transferred from the gel to a PVDF membrane (Bio-Rad) by electroblotting. The membranes were blocked using 5% skim milk in Tris-buffered saline containing 0.1% Tween-20 (TBST) at room temperature for 1 hour. The membrane was incubated with a specific primary antibody at 4°C overnight. On the next day, the membrane was washed 3 times with TBST and incubated with the secondary antibodies HRP (horseradish peroxidase)-conjugated for 1 hour at room temperature. Protein bands were visualized by exposing the membranes to an ECL (Enhanced Chemiluminescence) substrate for HRP-conjugated antibodies. The image acquisitions were performed on the ChemiDoc System to reveal and document the protein band.

2.8 TSP 2019

A pilot experiment conducted in 2019 was a 14-day study designed to test the payload systems under hypergravity conditions. In addition to its primary objective, the study took the opportunity to analyze the skeletal effects on mice hosted in the Mice Drawer System (MDS), which was originally constructed for microgravity environments. This allowed for an assessment of the MDS module's resilience to the centripetal forces experienced during the experiment. A total of 12 mice were involved in this study, with 6 of them placed in a hypergravity environment with a gravitational force of 3g, recapitulated by loading these cages on a large diameter centrifuge (LDC). The remaining 6 mice were kept in control cages.

The control cages (named training cages or MDS-ctrl) were constructed with the same dimensions and materials as the cages within the MDS module loaded on the LDC. C57BL/6J mice were used and male mice were exclusively chosen to avoid hormonal fluctuations and maintain consistency. At the end of the experiment mice were 5 month old. The mice diet remain the same during all experiment, administered in form of bars, whose composition is based on the animal's standard

diet. Additionally, Xanthan gum was added to the diet bars to maintain the food in the form of a 'biscuit'.

The 12 mice were trained for 14 days inside cages simulating the condition inside the MDS module, to allow them to take familiarity with the environment and the unusual administration of water and food. Afterwards, 6 of these mice were moved inside the MDS module, taken to ESTEC and left to rest for 2 days. The module was mounted on LDC and reached the 3 g condition in 2 hours.

This experiment is part of the Tissue sharing program (TSP) which sees various research groups from different parts of the world with their specific expertise.

The TSP was created with the aim of obtaining the greatest amount of information from each individual mouse by sharing different tissues, organs or sample between the different groups. For this purpose, the processing sequence also follows a precise order, in order to protect those organs more sensitive to degradation, like brain and muscles.

After the mouse is removed from the cage (or MDS), a series of steps are followed. Initially, there is a 5-minute observation of the mouse's immediate post-removal behavior. Urine is then collected and measured to record urinary output. Mouse is weighted and blood samples are obtained through retro-orbital plexus puncture with a Pasteur pipette. Finally, the mouse is euthanized.

After euthanasia, organs and tissues are collected, the head is separated from the body and the 2 parts move in parallel way. Various organs were collected from each group, then our last group was in charge of collecting the femur and the bone marrow. The bone marrow was flushed by using an insulin syringe, the suspension centrifuged at 300 g, surnatant and precipitated were collected and freeze in liquid nitrogen. Table 1 reports in detail how each tissue collected by our group was processed and analyzed.

TABLE 1 SAMPLE PROCESSING AND ANALYSIS OF TSP 2019

Sample/Tissue/Organ	Processing	Analysis
Blood	Collected in K3EDTA tubes	Analysis with veterinary instrument
Empty femur	Frozen in liquid nitrogen and then RNA extraction	Real time PCR
Femur bone marrow	Removal via insulin syringe	TBD

2.9 TSP 2023

FIG. 11 MOUSE INSIDE THE MDS CAGE

A second experiment was carried out in 2023, aiming to observe the long-term effects of exposure to hypergravity reaching 27 days of exposure. Also in this case the mice (11 for the 2 MDS modules) were trained in MDS payload to become familiar with the water and food supply systems. In total the experiment included 12 mice for hypergravity, but unfortunately due to an issue with the water delivery system, only 11 of the cages were fully operational during the experiment.

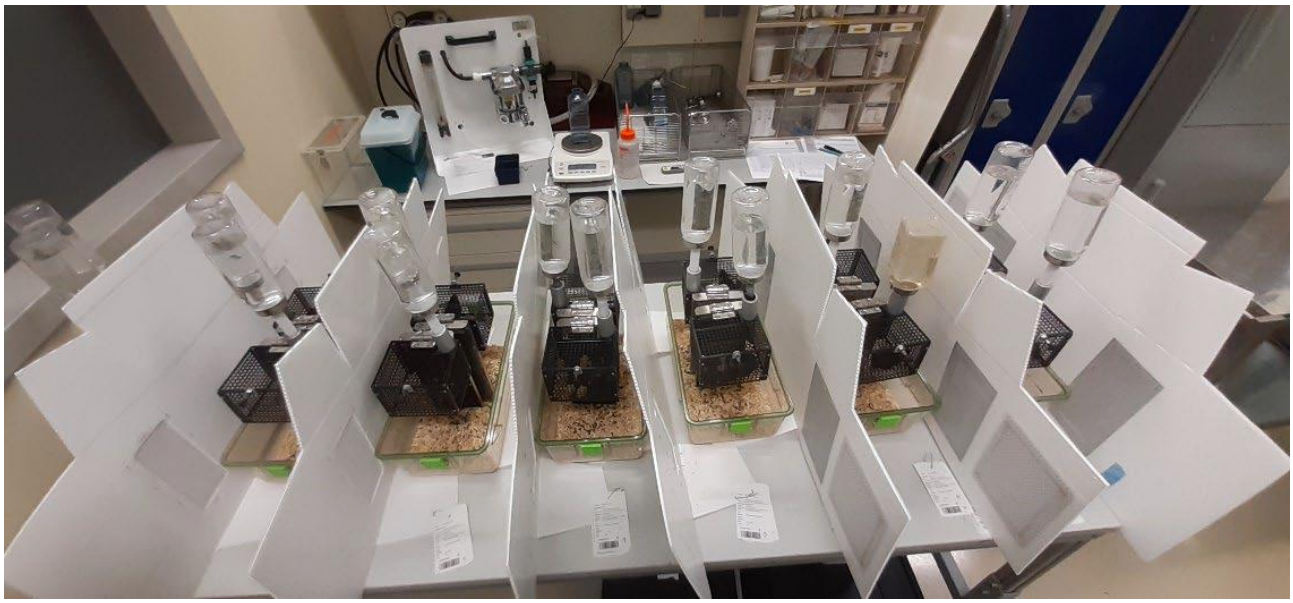

FIG. 12 MDS-CTRL MICE (TRAINING CAGES)

A second group of 12 mice was used for the control cages (MDS-ctrl) and a third group of 12 mice used as a control for cages (Vivarium). Only male mice were used for this experiment and the strain was C57BL/6J. At the end of the experiment mice were 5 month old. Food was based on the standard diet with the addition of Xanthan gum.

After 27 day of hypergravity exposure, mice were processed and analyzed following the same criteria of previous experiment. Once the mouse arrived at the bone team we proceed with the dislocation of the femur from the pelvis and tibia, and the tibia from the tarsus.

2.9.1 BEHAVIORAL STUDY

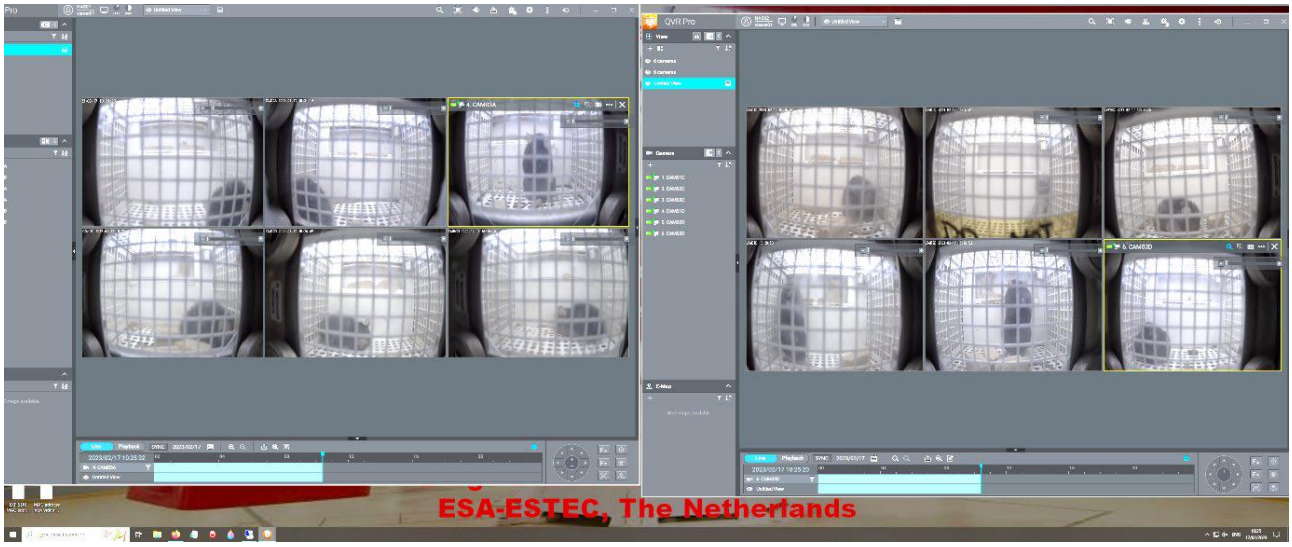

FIG. 13 MICE MONITORING THROUGH OBSERVATION SUBSYSTEM (OSS)

The mice were monitored during and after exposure in hypergravity. While the mice were exposed to hypergravity, it was possible to monitor their behavior through the Observation SubSystem (OSS) both during the day and at night. Furthermore, after the LDC stops and before the TSP their behavior was analyzed for approximately 5 minutes.

2.9.2 TSP SAMPLE TREATMENT

A distinction was made between right and left limb relative to the medial longitudinal axis of the mouse. As a result, right and left limb were processed and analyzed in a different way.

1. Right side: samples from the right side were frozen in liquid nitrogen and stored at -80°C.
    a. *Right femur*: the epiphyses were cut and the bone marrow flushed with an insulin syringe. The suspension was collected in a cryovial and centrifuged at 300 g for 5 minutes, the supernatant was collected and transferred to another cryovial and both pellet and supernatant frozen. The empty femur was also transferred into a clean cryovial and frozen.
    b. *Right tibia*: the epiphyses were cut, the bone marrow inside was removed, moved to a cryovial and frozen in liquid nitrogen.
2. Left side: samples from left side were fixed in 4% PFA and washed 3 times in PBS and stored at 4°C in PBS. Before final treatment, each sample was cleaned from muscle fragments and washed with PBS.

a. *Left femur*: moved into a tube with 5 mL of 4% PFA, left overnight and washed 3 times with PBS the next day (5 min between washes).
b. *Left tibia*: underwent the same treatment as the right one

The fibula was removed in both the right and left specimens.

The *spinal column* was finally processed, collecting the lumbar vertebrae number 1/2-3-4 and the spinal cord was removed. The 3rd vertebra was frozen in liquid nitrogen while the 1st and 2nd (they were left attached together) were moved in 4% PFA, then washed 3 times with PBS and stored in PBS. The 4th vertebra follow the same treatment of 1-2.

The *inner ears* and *calvaria* were removed from the dislocated head of the mouse.

The complete tissue collection for each mouse was done in 25-30 minutes.

Table 2 reports in detail how each tissue collected by our group was processed and analyzed.

TABLE 2 SAMPLE PROCESSING AND ANALYSIS OF TSP 2023

Sample/Tissue/Organ	Processing	Analysis
Blood	Eye sampling and blood moved in a vial with EDTA	Element HT5 (veterinary hematology analyzer)
Empty femur (R)	Frozen in N_2(l) and RNA extraction	PCR, RNAsec (on going)
Femur bone marrow (R)	Frozen in N_2(l)	TBD
Femur (L)	Fixation in PFA	MicroCT (preliminary results)
Empty tibia (R)	Frozen in N_2(l) and RNA extraction	PCR, RNAsec (on going)
Empty tibia (L)	Frozen in N_2(l)	Protein analysis
Lumbar vertebra n°1-2	Fixation in PFA	MicroCT (on going)

Lumbar vertebra n°3	Frozen in N_2(l) and RNA extraction	PCR, RNAsec (on going)
Lumbar vertebra n°4	Fixation in PFA	Hystology
Inner ear	Fixation in PFA	MicroCT (on going)
Calvaria	Fixation in PFA	MicroCT (on going)

2.9.3 MicroCT synchrotron Elettra

A preliminary investigation was conducted at the SYRMEP beamline (Synchrotron Radiation for MEdical Physics) of the Elettra synchrotron in Trieste. The scan was performed on 15 femurs, 15 internal ears, 15 calvariae and 15 vertebrae (5 for every condition). The samples were placed in ethanol and wrapped with parafilm and acquired with the high-resolution X-ray beam. The image was obtained through a scintillator and a camera. MicroCT scans of femurs were acquired with an average energy of 16.7 keV, inner ears and calvaria with 19.7 keV and finally the vertebrae with 23.6 keV. Most of the samples were acquired by collecting 1800 projections over 180 degrees. Bone volume (BV), total volume (TV) and the bone volume/total volume fraction (BV/TV) were estimated from the metaphysis. Bone volume (BV), total volume (TV) and bone volume/total volume fraction (BV/TV) and cortical thickness were estimated for the diaphysis.

2.10 REAL TIME PCR

RNA was extracted from cells (MLO-Y4) using Qiazol using the classic phenolic extraction protocol, while RNA extraction from TSP (tissue sharing program) samples of 2019 and 2023 was carried out using an Ultra Turrax T25 (IKA, potter) to pulverize the bones in liquid nitrogen. After nitrogen evaporation, lysing agent (Qiagen) was added. RNAeasy mini kit plus kit (Qiagen) was used for the extraction following the manufacturer's procedures. This protocol was applied to the femur, tibia and lumbar vertebra N°3.

RNA concentrations were measured at 260 nm using Nanodrop TM 1000 (Thermo Fisher Scientific, Waltham, MA, USA) and RNA purity and integrity was checked considering 260 nm/280 nm ratio with values included in the 1.8–2.1 range.

Samples from TSP experiment were also quantified with Tape Station 2200 (Agilent) with High Sensitivity RNA ScreenTape® (Agilent) in order to obtain the RIN value from each sample mandatory for the subsequent RNA seq analyses.

Complementary DNA (cDNA) synthesis was performed starting from 100 ng of total RNA and using the Qiagen QuantiTect Rev. Transcription Kit. The cDNA obtained was mixed with the appropriate amount Takyon™ Low ROX SYBR 2X MasterMix and primers (reverse and forward) and analyzed through Real-Time PCR (RT-PCR). The genes analyzed were: *Cx43* (connexin 43), *Bax* (bcl-2-like protein 4), *Bcl2* (B-cell lymphoma 2), *P53* (cellular p53), *P21* (cyclin-dependent kinase inhibitor 1), *P16* (cyclin-dependent kinase inhibitor 2A), *E11* (Podoplanin), *Lcn-2* (neutrophil gelatinase-associated lipocalin), *Ocn* (osteocalcin), *Sost* (sclerostin), *Opg* (osteoprotegerin), *Rankl* (receptor activator of nuclear factor kappa beta (NFkB ligand) and *Ppar gamma* (proliferator-activated receptor γ).

The housekeeping gene *Gapdh* was used as the endogenous control for normalization. Data were reported as ratio GENE/GADPH, which represents the expression of the gene of interest divided by the expression of *Gapdh* in the same sample. The gene expression was calculated with 2^ (-ΔCt) method and expressed as fold change referred to the control.

2.11 STATISTIC

Data were analyzed with GraphPad Prism 9.3 software (GraphPad Software, Inc., San Diego, CA, USA) and are expressed as mean ± standard deviation (S.D.). Student t-test with Welch correction and one way-ANOVA was used. Level of significance was set at $p<0.05$ (*$p<0.05$, **$p<0.01$, ***$p<0.001$, ****$p<0.0001$).

3.0 RESULTS

3.1 LOW-DOSE OF LCN-2 STIMULATION INDUCED OVEREXPRESSION OF SENESCENCE-RELATED GENES IN MLO-Y4 OSTEOCYTES

We recently reported that the secreted protein Lipocalin-2 (LCN-2) is expressed in bone and has a role in skeleton development and bone remodeling. Additionally, LCN-2 was found to be over-expressed in simulated microgravity animal models[59], which are known to develop osteopenia. This suggests that LCN-2 may contribute to the bone loss associated with microgravity condition. It has well-documented that osteopenia, observed following spaceflights, might also be attributed to osteocyte apoptosis[18,19,60]. To enhance our understanding of the mechanisms and pathways influenced by LCN-2 in bone, we evaluated the effects of LCN-2 stimulation in osteocytes.

A preliminary experiment, aimed at the investigating the potential impact on apoptosis and cellular senescence, involved culturing murine osteocyte MLO-Y4 cell line for five days. Following this period, the cells were treated with different concentrations of LCN-2 ranging from 100 to 500 ng/ml. The preliminary results showed that alteration in the expression of genes associated with senescence and apoptosis were observable following treatment with LCN-2 at a concentration of 200 ng/ml (data not shown).

Based on these preliminary findings, we further explored the impact of LCN-2 on the apoptosis and senescence of osteocytes. This was accomplished by culturing MLO-Y4 for five days and treating them with 200 ng/ml LCN-2 in the final 8h of the assay. A negative control, which was not treated, was also included. Expression of bone homeostasis-, apoptosis- and senescence-related genes was evaluated (Fig.14) by Real Time PCR.

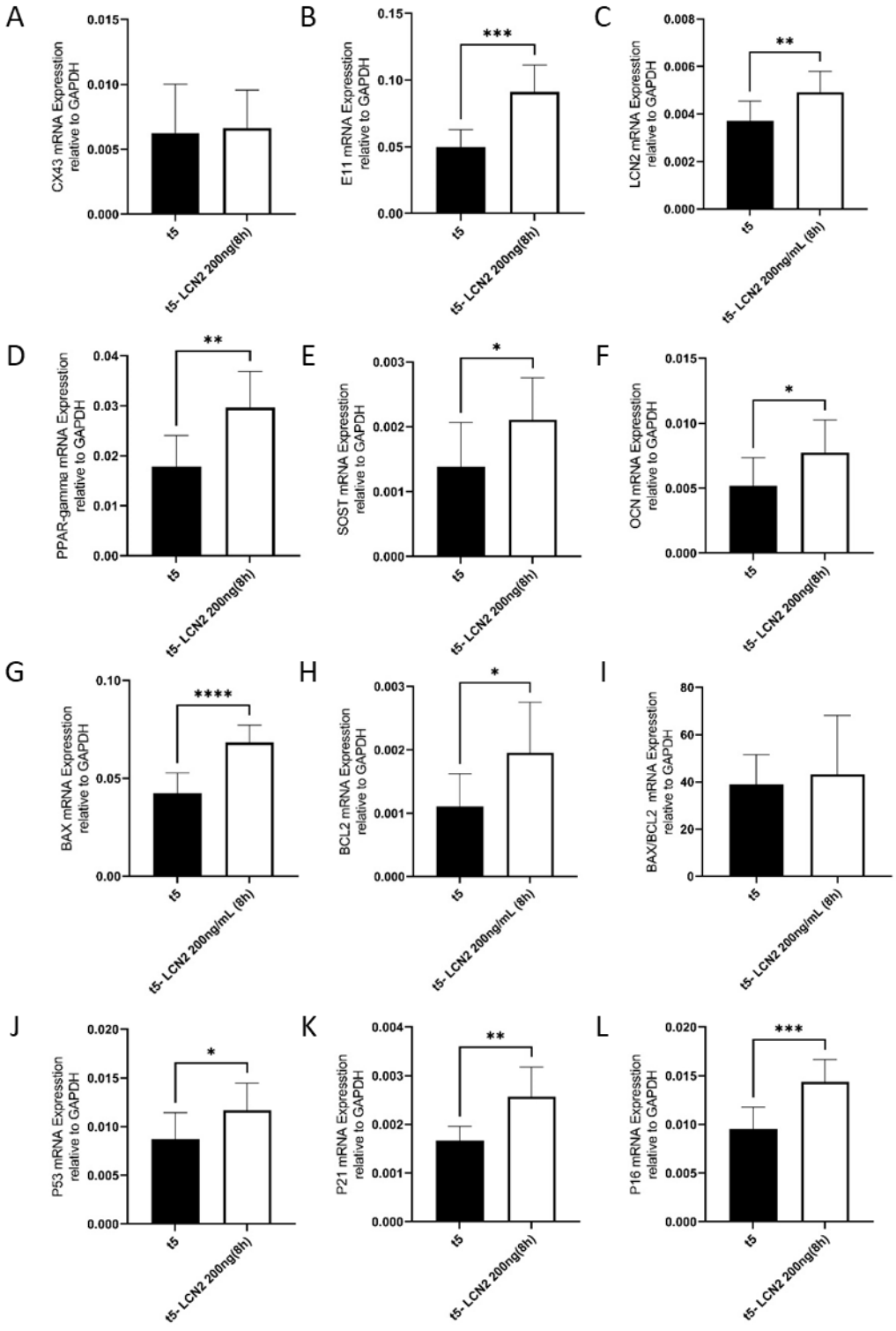

FIG. 14 MLO-Y4 GENE EXPRESSION AFTER 200NG/ML LCN-2 STIMULATION EXPERIMENT WAS PERFORMED AS DOUBLE EXPERIMENT (N=5). DATA ARE SHOWN AS MEAN ± S.D, T-TEST WITH WELCH CORRECTION, (*) P<0.05, (**) P<0.01, (***) P<0.001. *CX43*: CONNEXIN 43 (A), *E11*: PODOPLANIN (B), *LCN-2* LIPOCALIN-2 (C), *PPARGAMMA*: PEROXISOME PROLIFERATOR-ACTIVATED RECEPTOR GAMMA (D), *SOST*: SCLEROSTIN (E), *OCN*: OSTEOCALCIN (F), *BAX*: BCL2 ASSOCIATED X (G), *BCL2*: B-CELL CLL/LYMPHOMA 2 (H), *BAX/BCL2* RATIO (I) APOPTOSIS REGULATOR, *P53*: PROTEIN 53 (J), *P21*: CYCLIN-DEPENDENT KINASE INHIBITOR 1 (K), *P16*: CYCLIN-DEPENDENT KINASE INHIBITOR 2A (L).

Transcription levels of typical osteocyte markers *Cx43* and *E11* were firstly evaluated. Connexin-43 (CX43) is a transmembrane protein, which acts as an intercellular channel, modulating the response to hormone and mechanical stimuli between bone cells. It is the most abundant gap junction protein in bone, and it has been reported as an integral component of skeletal homeostasis[61]. Expression of *Cx43* was not affected by LCN-2 stimulation (Fig 14-A).

In addition, mRNA levels of *E11* were investigated. *E11* (or gp38/Podoplanin) is a gene highly expressed by MLO-Y4 cell line and it is associated with the formation-elongation processes of dendrites in osteocytes. E11 is the earliest osteocyte-selective protein to be expressed when osteoblasts differentiate into osteoid cells or osteocytes, during dendritic formation[62]. Interestingly, LCN-2 stimulation resulted in a significant overexpression of *E11* (Fig 14-B) compared to the untreated control group ($p \leqslant 0.001$).

Stimulation with LCN-2 also led to an increase in the expression of the *Lcn-2* gene itself (Fig 14-C), in comparison with the negative control ($p \leqslant 0.01$). This data agrees with recent evidence showing that the addition of LCN-2 to the cells led to an increase in endogenous *Lcn-2* mRNA[63].

Expression of bone homeostasis-related genes, such as *Ppar-gamma*, *Sost* and *Ocn* was also evaluated. *Ppar-gamma* is primarily an important marker of adipose tissue[64]. Less is known about its role in bone physiology, where it appears to act as a negative regulator of bone formation by suppressing osteoblastogenesis from bone marrow-derived cells[65]. *Ppar-gamma* was found upregulated (Fig 14-D) in LCN-2 stimulated osteocytes compared to negative control ($p \leqslant 0.01$), suggesting that LCN-2 might induce bone remodeling and readaptation using also PPAR-gamma pathway. As a confirmation of this hypothesis, *Sost/Sclerostin* showed a similar trend (Fig 14-E), being significantly induced by stimulation with LCN-2 compared to control ($p \leqslant 0.05$). *Sost* is indeed a gene highly expressed by mature osteocytes and it contributes to bone homeostasis by regulating both osteoclastogenesis and osteoblast differentiation and activity[66,67]. Conversely, LCN-2 stimulation also induced an up-regulation of *Ocn* (Fig 14-F) ($p \leqslant 0.05$) when compared to the negative control. Osteocalcin is a gene characteristically expressed by osteoblasts, yet it is typically downregulated during the transition from the osteoblast to the osteocyte stage. [68].

The apoptosis-related genes *Bax* and *Bcl-2* were examined. *Bax* was up regulated upon stimulation with 200 ng/ml LCN-2 (Fig 14-G) ($p \leq 0.0001$), when compared to the negative control, suggesting a

possible role of LCN-2 in the initiation of apoptosis. BAX (Bcl-2-associated X protein), a pro-apoptotic factor, is known to migrate to the mitochondria in response to apoptotic signals, determining the cytochrome c release [69]. On the other hand, *BCL-2* was upregulated by LCN-2 treatment as well (Fig 14-H) ($p \leqslant 0.05$ compared to negative control), showing a two-times fold increase compared to the control levels. The role of antiapoptotic proteins such as BCL-2 is to inhibit their pro-apoptotic counterparts, thereby creating an actual rheostat whose balance determines the fate of the cell[70]. Consequently, BCL-2's regulatory role involves binding with other proteins of the BCL-2 family, such as BAX and BAK, to prevent the release of cytochrome C from the mitochondria [71].

In this case, *Bax/Bcl2* ratio was evaluated to determine whether the gene expression levels of these two antagonistic behaving genes are towards a pro-apoptotic (*Bax*) or anti-apoptotic (*Bcl-2*) pathway. The ratio between *Bax* and *Bcl-2* expression represents a cell death switch, which determines the life or death of cells in response to an apoptotic stimulus. An increased *Bax/Bcl2* ratio decreases the cellular resistance to apoptotic stimuli, leading to increased cell death[72]. Interestingly, although *Bax* is highly upregulated (Fig 14-I), no statistically significant difference in the *Bax/Bcl2* ratio was observed between control and LCN-2 treatment.

Finally, expression of senescence-related genes was also analyzed. P53, P21 and P16 are cell cycle regulators, and are recognized as senescence markers[73]. Notably, an overexpression of *P53*, *P21* and *P16* was observed after LCN-2 stimulation (Fig 14-J-K-L), in comparison with negative control ($p \leqslant 0.05$, $p \leqslant 0.01$ and $p \leq 0.001$, respectively), suggesting a possible role of LCN-2 in promoting cellular senescence.

Taken together these results indicate that osteocytes did not undergo apoptosis after LCN-2 stimulation in this cell culture conditions, but might enter in a senescence phase. As a confirmation, the cellular corresponding apoptotic event was also analyzed by TUNEL assay, showing no significant difference in apoptotic cell number, between LCN-2 stimulation and control group (data not shown).

3.2 SIMULATED-MICROGRAVITY INDUCED LIPOCALIN-2 OVEREXPRESSION IN SERUM OF TAIL-SUSPENDED MICE IN HLU

The decreased mechanical loading of weight-bearing bones caused by microgravity in space leads to bone loss in humans during space travels[74,75]. Although spaceflight experiments are certainly the most physiologically relevant method of studying μ*g*-induced bone loss, they come with significant

limitations. Therefore, several ground-based methods have been developed to subject cells or animals to near-µ*g* conditions. The hindlimb unloading (HLU) model is the most common method to simulate spaceflight conditions in rodents, where rats or mice are suspended by their tails. We also reported that transgenic mice over-expressing LCN-2 exhibited osteopenia, comparably to the one normally observed in HLU models[76]

Based on these considerations, an HLU experiment was conducted in collaboration with the group of Prof. Maria Grano from the University of Bari, where both male and female mice were kept in tail suspension for 4 weeks. A control group of not tail-suspended mice was also included in the study. After 4 weeks, blood serum of both conditions was collected and protein levels of Lipocalin-2 (LCN-2) were analyzed by ELISA.

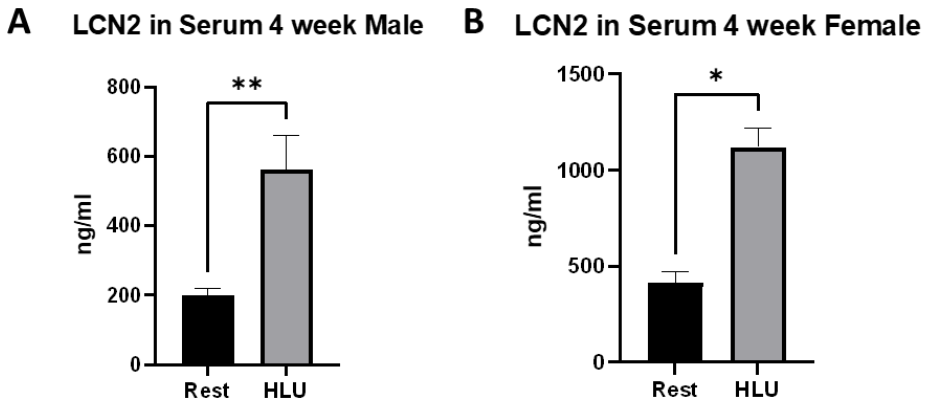

FIG. 15 SERUM LCN-2 CONCENTRATION IN 4 WEEKS OF HLU EXPOSURE IN MALE (A) AND FEMALE MICE (B). EXPERIMENT WAS PERFORMED ONE TIME (N=3). DATA ARE SHOWN AS MEAN ± S.D. T TEST WITH WELCH CORRECTION. (*) P<0.05, (**) P<0.01.

ELISA assay showed a significant increase of LCN-2 expression in tail-suspended mice (~1,000 ng/ml) compared to the control Rest group in both male ($p<0.01$) (Fig.15-A) and female ($p<0.05$) (Fig.15-B) mice. These data suggested that LCN-2 could be a biomarker of osteopenia in simulated-µ*g* condition.

3.3 HIGH-DOSE OF LCN-2 STIMULATION DID NOT INDUCE APOPTOSIS IN MLO-Y4 OSTEOCYTES

Based on the results of previous experiments, a second *in vitro* experiment was performed by stimulating osteocytes with 1000 ng/ml LCN-2, to investigate whether LCN-2 effects were dose

dependent. The LCN-2 concentration was selected based on ELISA results of HLU experiment in mice, showing a serum concentration of LCN-2 close to 1000 ng/ml in tail-suspended mice.

MLO-Y4 cells were seeded and cultured for 48h, prior the treatment with 1000 ng/ml LCN-2 for 48h. A negative control was also carried out, maintaining cells in standard culture medium.

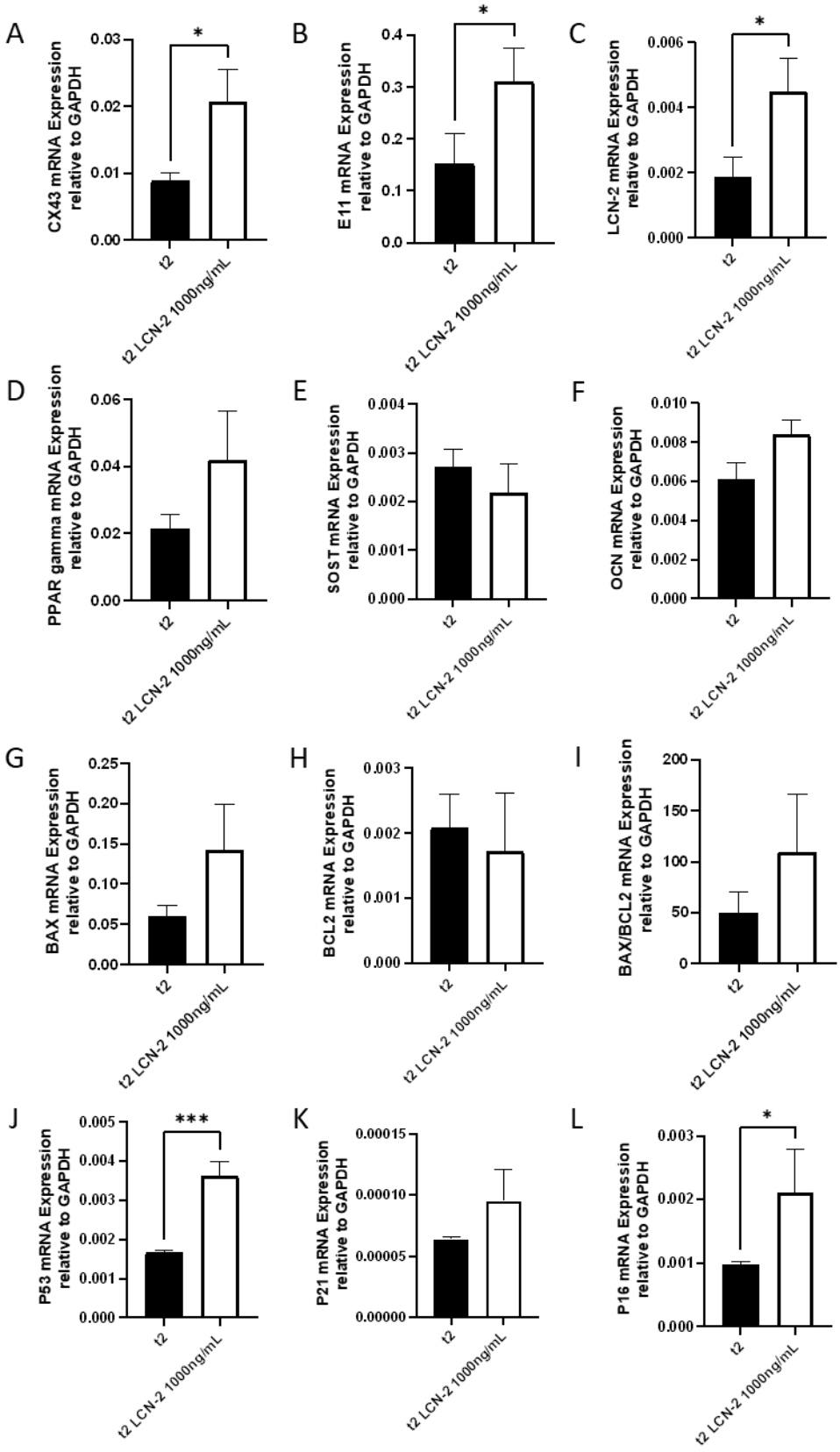

FIG. 16 GENE EXPRESSION AFTER 1000NG/ML LCN-2 STIMULATION. EXPERIMENT WAS PERFORMED AS SINGLE EXPERIMENT (N=3). DATA ARE SHOWN AS MEAN ± S.D, T-TEST, (*) P<0.05, (**) P<0.01, (***) P<0.001. *Cx43*: CONNEXIN 43 (A), *E11*: PODOPLANIN (B), *LCN-2* LIPOCALIN-2 (C), *PPAR-GAMMA*: PEROXISOME PROLIFERATOR-

ACTIVATED RECEPTOR GAMMA (D), *SOST*: SCLEROSTIN (E), *OCN*: OSTEOCALCIN (F), *BAX*: BCL2 ASSOCIATED X (G), *BCL2*: B-CELL CLL/LYMPHOMA 2 (H), *BAX/BCL2* RATIO (I) APOPTOSIS REGULATOR, *P53*: PROTEIN 53 (J), *P21*: CYCLIN-DEPENDENT KINASE INHIBITOR 1 (K), *P16*: CYCLIN-DEPENDENT KINASE INHIBITOR 2A (L).

Transcriptional levels of bone homeostasis-, apoptosis- and senescence-related genes were evaluated as described above.

Contrary to previous experiment, *Cx43* was significantly upregulated after 1000 ng/ml LCN-2 treatment, compared to the control (Fig 16-A) ($p \leqslant 0.05$), suggesting a dose dependent effect correlation. On the other hand, both *E11* (Fig 16-B) and *Lcn-2* (Fig 16-C) were overexpressed after 1000 ng/ml LCN-2 treatment compared to the control ($p \leqslant 0.05$ in both cases), in accordance with experiment at lower dose.

Contrary to previous results, no significant difference was observed in the expression of *Ppar-gamma* (Fig 16-D), *Sost* (Fig 16-E) and *Ocn* (Fig 16-F) after stimulation with 1000 ng/ml LCN-2 in comparison with the control.

Furthermore, also *Bax* (Fig 16-G) expression showed a slight not significant increase after 1000 ng/ml LCN-2 treatment compared to control.

Interestingly, contrary to 200 ng/ml LCN-2 stimulation, *Bcl-2* (Fig 16-H) was not modulated after 1000 ng/ml LCN-2 stimulation in comparison with the control. As a result, *Bax/Bcl2* ratio (Fig 16-I) showed a slight not significant increase after 1000 ng/ml LCN-2 treatment compared to the control. However, this increase was not sufficient to induce cellular apoptotic event, as evidenced by the negative results of a subsequent TUNEL assay (data not shown).

The senescence genes *P53* (Fig 16-J) ($p \leqslant 0.001$ compared to control) and *P16* (Fig 16-L) ($p \leqslant 0.05$ compared to control) exhibited a comparable trend with previous experiment, while *P21* (Fig 16-K) showed an upregulation in LCN-2 group, but not statistically significant. Unfortunately, in this experiment, we only conducted a triplicate instead of the usual quintuplicate, and therefore it will need to be repeated to determine if a statistically significant difference can be observed.

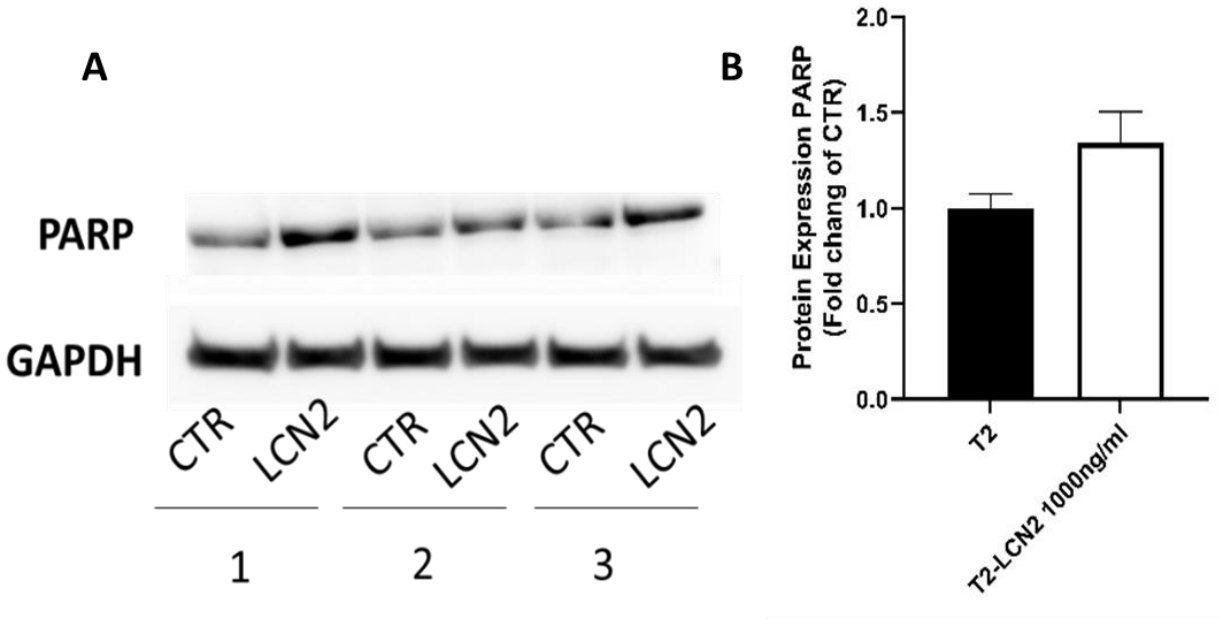

FIG. 17 WESTERN BLOT ANALYSIS (A) AND QUANTIFICATION OF PARP (B). DENSITOMETRIC ANALYSIS SHOWN AS MEANS ± SD OF THREE REPLICATES OF PARP.

However, a Western blot analysis on PARP-1 protein was also performed, confirming that apoptotic pathway was not activated after 1000 ng/ml LCN-2 stimulation. The lack of band at lower molecular weight suggest indeed that PARP-1 cleavage, an essential event of the apoptotic cascade, did not occur. Taken together, these data confirm that LCN-2 stimulation did not induce apoptotic process in MLO-Y4 osteocyte, neither at low or high dose.

3.4 LCN-2 STIMULATION DID NOT INDUCE MITHONDRIAL IMPAIRMENT IN MLO-Y4 OSTEOCYTES

To further investigate whether LCN-2 may induce osteocyte function impairments, mitochondrial function was evaluated. Microgravity-induced bone loss is indeed often associated with oxidative stress and dysregulation of mitochondrion homeostasis[77,78]. MLO-Y4 cells were treated with 1000 ng/ml LCN-2 for 48h or maintained in standard culture medium as control. Mitochondrial metabolism was evaluated by measuring the Oxygen Consumption Rate (OCR) using Seahorse.

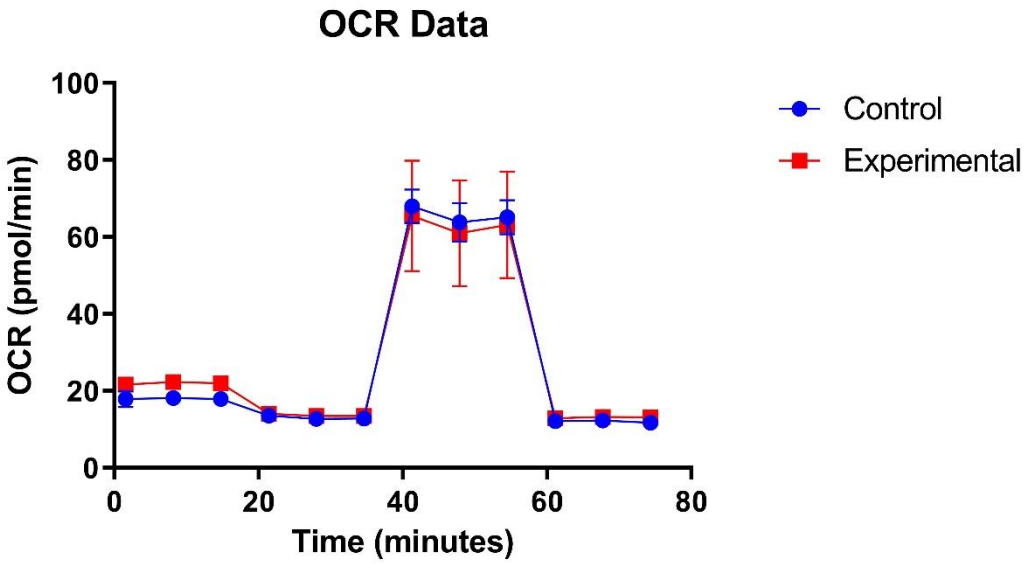

FIG. 18 MITOCHONDRIAL STRESS TEST IN MLO-Y4 OSTEOCYTES CELLS. OCR WAS MEASURED AFTER TREATMENT 1000 NG/ML LCN2 FOR 48 H FOLLOWED BY CONSECUTIVE INJECTIONS OF OLIGOMYCIN (1.5 MM), FCCP (1 MM), AND ANTIMYCIN A (0.5 MM)/ROTENONE (0.5 MM). THE EXPERIMENT WAS PERFORMED ONE TIME (N=3). DATA ARE SHOWN AS MEAN ± S.D.

Results showed that no significant differences in OCR can be observed between the control and the treated sample, indicating that LCN-2 stimulation, at that dose, did not induce any damage to the mitochondrial oxidative phosphorylation process. An effect on the mitochondria would result indeed in a drop of OCR values in the graph, in the area between 40 and 60 minutes, when an ATP synthase inhibitor (FCCP) is added to the cells.

3.5 EFFECT OF RPM AND LCN-2 STIMULATION IN MLO-Y4 OSTEOCYTES

To assess a potential synergistic effect between LCN-2 and microgravity, the entire experiment was also carried out in conditions of simulated microgravity. MLO-Y4 cells were cultured for 5 days and then treated with 200 ng/ml LCN-2 for the last 8 h of experiment or left in standard culture medium

as control. The experiment was performed in RPM machine, for microgravity simulation. A ground control was also performed, and gene expression was evaluated by real time PCR, in all the experimental groups (Fig. 19).

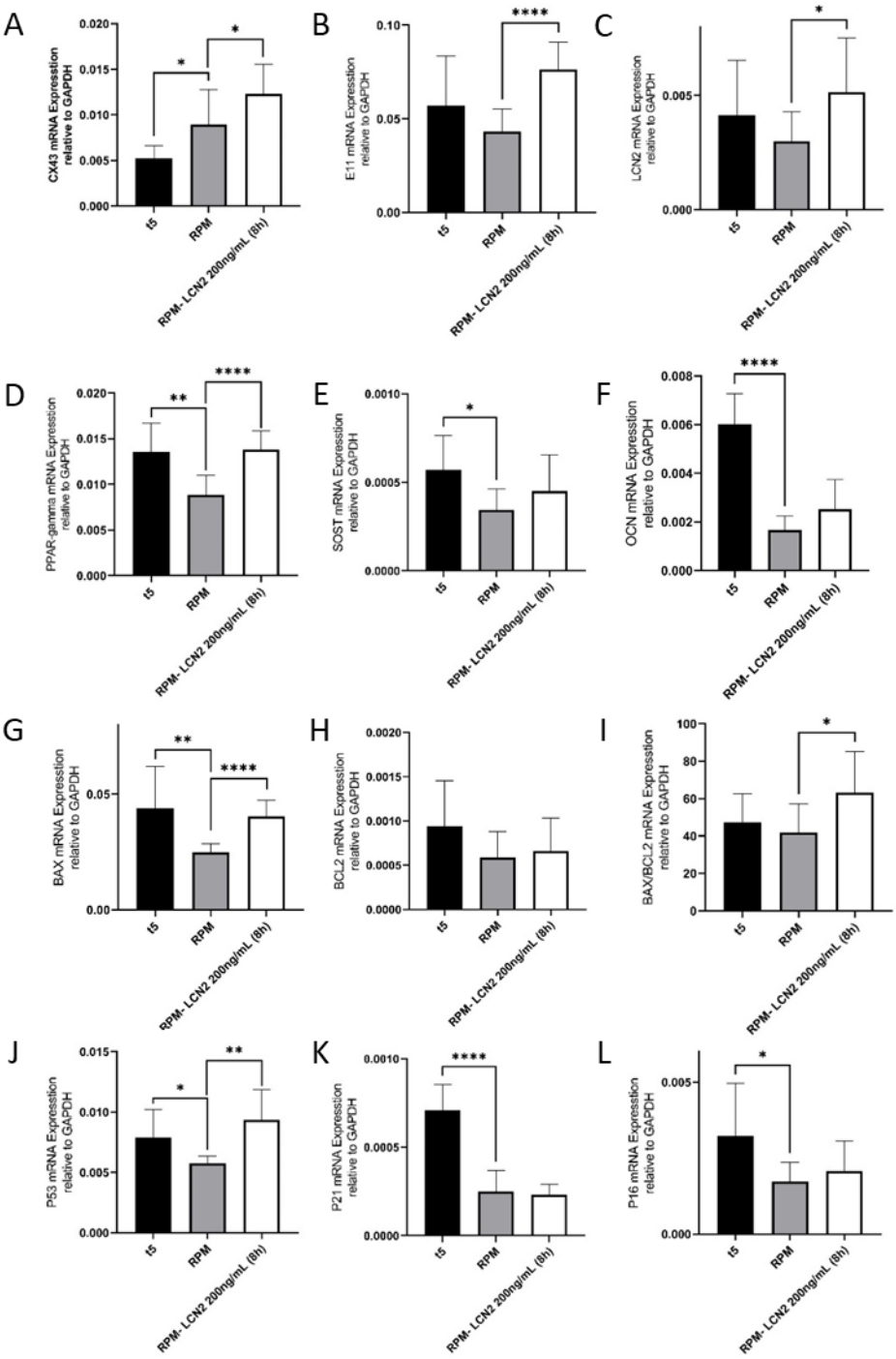

FIG. 19 GENE EXPRESSION AFTER STIMULATION IN RPM WITH LCN-2 200 NG/ML. EXPERIMENT WAS PERFORMED AS DOUBLE EXPERIMENT (N=5). DATA ARE SHOWN AS MEAN ± S.D, ONE-WAY ANOVA WITH WELCH CORRECTION, (*) P<0.05, (**) P<0.01, (***) P<0.001 E (****) P<0.0001. *Cx43*: CONNEXIN 43 (A), *E11*: PODOPLANIN (B), *LCN-2* LIPOCALIN-2 (C), *PPAR-GAMMA*: PEROXISOME PROLIFERATOR-ACTIVATED RECEPTOR GAMMA (D), *SOST*: SCLEROSTIN

(E), *Ocn*: Osteocalcin (F), *Bax*: BCL2 Associated X (G), *Bcl-2*: B-Cell CLL/Lymphoma 2 (H), *Bax/Bcl-2* ratio (I) Apoptosis Regulator, *P53*: Protein 53 (J), *P21*: cyclin-dependent kinase inhibitor 1 (K), *P16*: cyclin-dependent kinase inhibitor 2A (L).

Cx43 was found upregulated in simulated-µ*g* (RPM) compared to the control group (Fig.19-A) (p≤0.05). Furthermore the stimulation with LCN-2 in RPM also determined a significant increase in *Cx43* expression in comparison with RPM alone (p≤0.05 RPM LCN-2 *vs.* RPM), suggesting that simulated microgravity increases the effect of LCN-2, contrary to the ground experiment.

E11 expression was not affected by simulated microgravity, while LCN-2 treatment in RPM determined an increase in *E11* expression (Fig.19-B) (p≤0.0001 RPM LCN-2 *vs.* RPM), confirming the effect of LCN-2 previously observed.

The same trend was observed on *Lcn-2* mRNA levels (Fig.19-C), where the presence of the same protein triggers a positive feedback effect, leading to a higher expression of endogenous LCN-2 (p≤0.05 RPM LCN-2 *vs.* RPM), as already noticed in ground experiment.

In addition, RPM induced a downregulation of both *Ppar-gamma* (Fig.19-D) and *Sost* (Fig.19-E) (p≤0.01 and p≤0.05 RPM *vs.* ground control, respectively). Furthermore, LCN-2 stimulation in simulated microgravity induced an overexpression of *Ppar-gamma* to restore control levels, confirming the effect of LCN-2 previously observed. Intriguingly, *Ocn* (Fig.19-F) was strongly downregulated in simulated-µ*g* (p≤0.0001 RPM *vs.* ground control) and no significant difference was detected after LCN-2 stimulation.

Expression of apoptotic genes was evaluated and *Bax* (Fig.19-G) was found less expressed in simulated microgravity conditions compared to ground control (p≤0.01 Ctrl *vs.* RPM), while LCN-2 treatment in RPM restored *Bax* expression to ground control levels (p≤0.0001 RPM LCN-2 *vs.* RPM). The expression of *Bax* partially disagrees with what is reported in literature, where an exposure to both real and simulated microgravity would lead to an increase in this gene in bone cells[79,80].

On the contrary, *Bcl-2* (Fig.19-H) transcriptional levels were not affected by neither microgravity nor subsequent LCN-2 stimulation. However, although *Bax/Bcl2* (Fig.19-I) ratio was not modulated by simulated microgravity in comparison with ground control, a synergic effect of LCN-2 and microgravity may be hypothesized. *Bax/Bcl2* ratio was indeed increased after LCN-2 stimulation in

RPM, suggesting a possible effect in apoptosis induction. Further experiments are ongoing to confirm this data.

The senescence-related gene *P53* (Fig.19-J) showed a statistically significant downregulation in RPM ($p \leq 0.05$ RPM *vs.* ground control) compared to ground control. Similarly to *Bax*, stimulation with LCN-2 brought *P53* expression back to ground control levels ($p \leq 0.01$ RPM LCN-2 *vs.* RPM).

Finally, both *P21* (Fig.19-K) and *P16* (Fig.19-L) were downregulated in RPM compared to ground control ($p \leq 0.0001$and $p \leqslant 0.05$ RPM *vs.* ground control, respectively). Moreover, LCN-2 stimulation in RPM did not affect their expression, which was comparable to RPM control.

3.6 TSP 2019: EFFECTS OF 14-DAY EXPOSURE TO HYPERGRAVITY (3G)

In parallel with *in vitro* studies investigating the role of microgravity and LCN-2 in bone cells, an experiment was conducted under hypergravity conditions to act as a paradigm and highlight genes sensitive to altered gravity. Furthermore, this study aimed to determine whether hypergravity could improve bone physiology. For this purpose, a payload named MDS originally designed for microgravity experiments was utilized. A first preliminary experiment was conducted to investigate whether the payload could also be adapted for the opposite condition: hypergravity. After a dry run without any animals inside, we tested the payload for 14 days in 3g with six animals inside (MDS-3g). A control was also carried out (MDS-ctrl), by maintaining 6 mice in control cages.

The choice to use 3 g is related to several findings[81,82] In particular, Bojados and Jamon found that in male C57Bl6/J mice hypergravity acted as endurance training on muscle strength up to 3 g, while becoming deleterious at 4 g [83,84]. Moreover, in a previous paper, we demonstrated that exposure to 2g for three months enhanced bone architecture and bone cell activity[44]. Similarly, Gnyubkin V. et al observed a positive impact on bone after 21 days of 2g exposure, but a detrimental effect was seen with 3g exposure[84].

MDS-3g cages were loaded onto the LDC and 3g gravitational force was reached after 2 hours. The temperature inside each cage was monitored over time, showing an average value of 25 degrees and a relative humidity between 60-70%. These values according to the Guide for the Care and Use of Laboratory Animals, are in the recommended ranges that are for dry-bulb temperature and humidity 18–26°C and 30–70%, respectively[85]. Mice were numbered with the following coding: a

first number indicating the MDS module (1 in this case), followed by a second number indicating the cage inside the module (1-2-3-4-5-6).

Water consumption was monitored during all the experiment, as a measurement of the mice wellness. Water consumption showed a drastic drop during in the first days of the experiment in the centrifuge (Fig.20-A). Due to this, the g force was reduced from 3g to 2g for 24 h, to allow mice adaptation. Gravity value was reset on the pre-established values (3g) the following day. Unfortunately, one of the 6 mice (mouse 1.5) continued to consume an insufficient amount of water after 7 days, leading to the suspension of the experiment and euthanasia for the said mouse. Mice were weighted at the beginning and at the end of the experiment and all of them showed a weight decrease by approximately 10-20% compared to the initial weight in hypergravity (Fig.20-B).

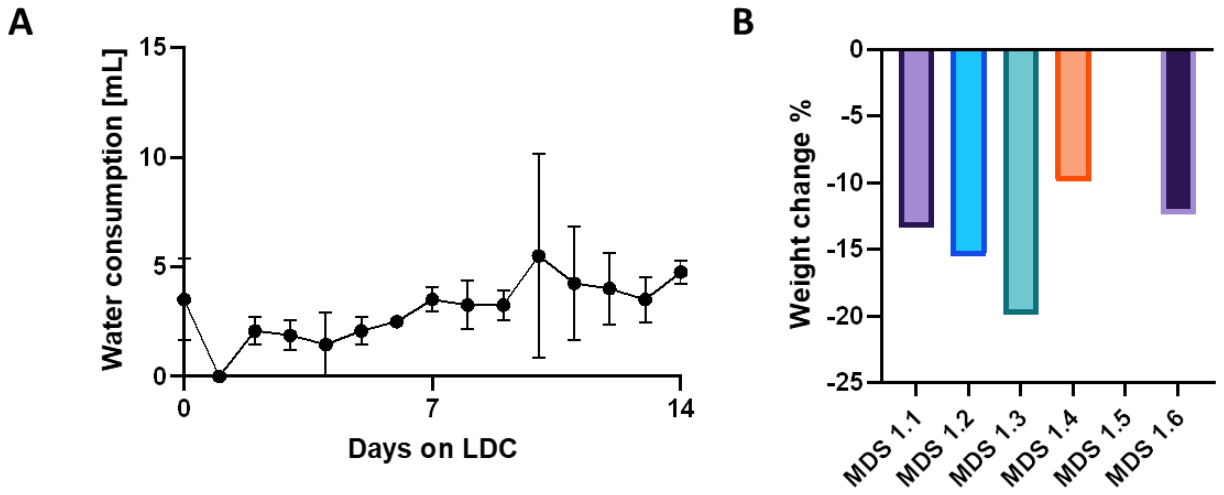

FIG. 20 WATER CONSUMPTION (ML) OF MICE FROM 3G EXPERIMENT DURING EACH DAY (A) AND PERCENTAGE OF WEIGHT CHANGES OF 3G MICE BETWEEN THE BEGINNING AND THE END OF THE EXPOSURE (B). THE VALUES ARE EXPRESSED AS AVERAGE ± SD.

3.1.1 Hypergravity determined an increase in red blood cells and decrease in white blood cells

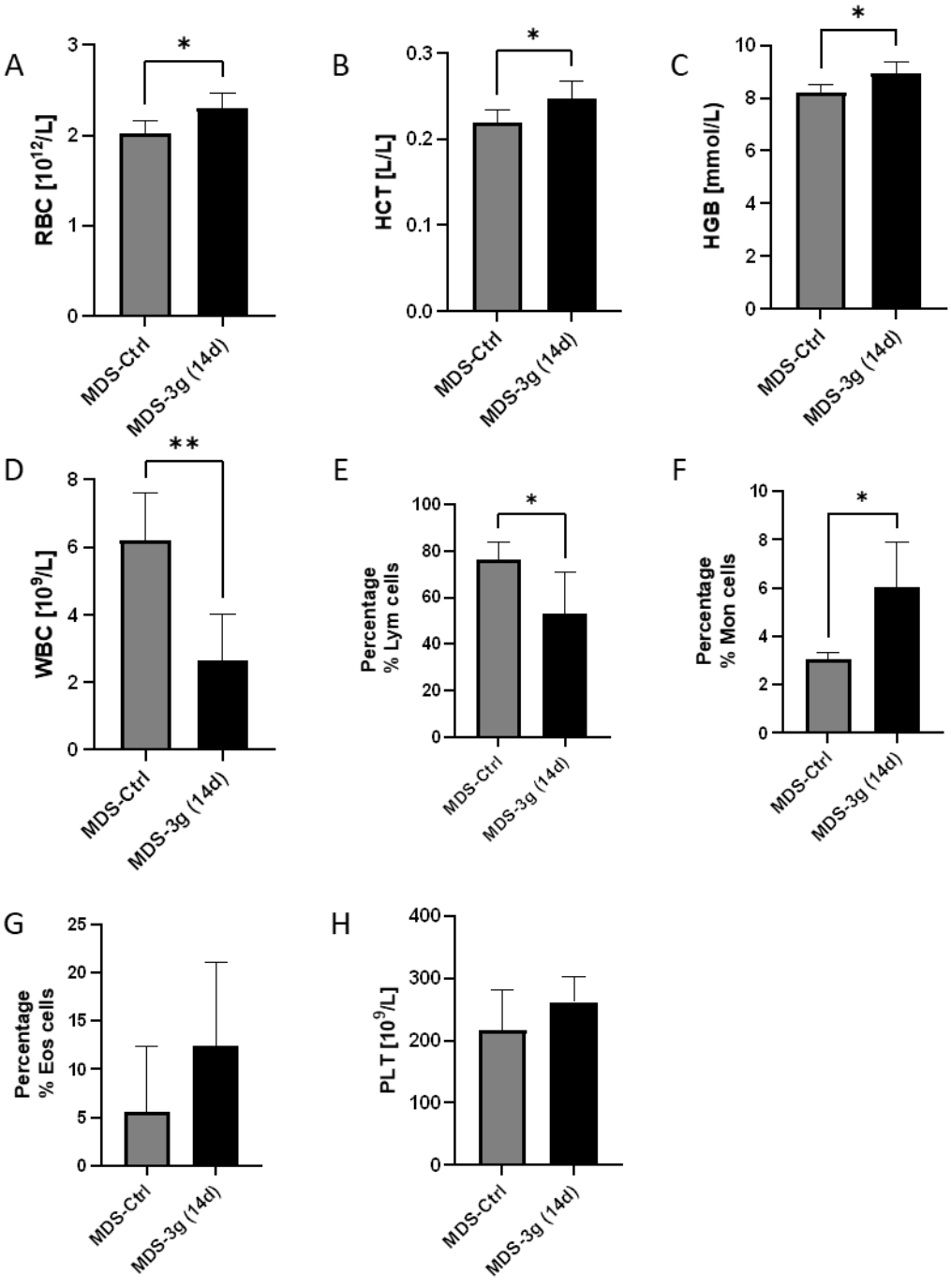

Fig. 21 Blood analysis of mice from 14-day 3g exposure. RBC: Red blood cells (A), HCT: Hematocrit (B), HGB: Hemoglobin (C), WBC: White blood cells (D), Lym: lymphocytes (E),Mon: Monocytes (F), EOS: Eosinophil (G) and PLT: Platelet (H). Data are shown as mean ± S.D, t- test with Welch correction, (*) p<0.05, (**) p<0.01, (***) p<0.001.

TABLE 3 BLOOD PARAMETERS (SOURCE: CHARLES RIVER). DATA ARE SHOWN AS MEAN ± S.D.

	Low	High	MDS-Ctrl	MDS-3g (14d)
WBC 10^9/L	4.45	13.96	6.21±1.26	2.64±1.22
LYM %	61.26	87.18	76.1±7	53.1±15.67
MON %	2.18	11.02	3.05±0.28	6.04±1.66
(EOS %) %	0.13	4.42	5.58±6.18	12.38±7.79
RBC 10^{12}/L	7.14	12.20	2.02±0.12	2.31±0.14
HGB mmol/L	6.7	11.92	8.20±0.28	8.93±0.41
HCT L/L	0.373	0.620	0.21±0.01	0.25±0.02
PLT 10^9/L	841	2159	142.7±61.9	262.2±36.3

After the mouse was removed from the MDS, and before euthanasia, blood samples were obtained, under anesthesia, through retro-orbital plexus puncture with a Pasteur pipette. Different blood parameters were analyzed and Table 3 reports a summary with all the values obtained and the reference values for a better understanding (source: Charles River). From the table, it was evident that our animals had values different from the reference values of Charles River. The laboratory that provided us with the service, possessed analytical tools designed for larger animals than mice, specifically dogs and cats. While they assured us of the accuracy of the analyses, they recommended that we focused not on absolute values, but rather on relative values between treated and untreated groups.

A statistically significant increase in red blood cells (RBC), in hematocrit and hemoglobin in MDS-3g compared to MDS-ctrl was noticed ($p \leq 0.05$ in all the conditions) (Fig.21-A).

Furthermore, blood analysis highlighted an even more significant decrease in white blood cells (WBC) in MDS-3g compared to MDS-ctrl ($p \leq 0.01$) (Fig.21-D). The effect on different subgroups of WBC was also investigated, showing a significant reduction in percentage of lymphocytes when mice are exposed to hypergravity ($p \leq 0.05$ compared to control group). Since lymphocytes constitute the main cell type among WBC, it is reasonable to expect a drop in their number leading to a drop also in the overall WBC number. The decrease in lymphocytes and therefore in WBC could therefore be tailored to stress factors due to the experiment itself [86]. Monocytes subgroup showed an opposite trend, with a significant increase in MDS-3g compared to MDS-ctrl ($p \leq 0.05$). In addition, eosinophil

percentage was also analyzed. The eosinophil is well recognized as a central effector cell in the inflamed asthmatic airway [87]. In this experiment, no statistically significant difference was found between MDS-3g and MDS-ctrl, but the average value on MDS-3g was outside the normal range (Table 3).

Finally, platelets showed values lower than the standard parameters and a slight increase compared to the MDS-ctrl, even if not statistically significant.

3.1.2 GENE EXPRESSION

After euthanasia, femurs were isolated, bone marrow was flushed out, and RNA extraction was performed from the empty bone devoid of the epiphysis. Gene expression was evaluated in order to define potential effects of hypergravity on skeletal system. In particular *Ocn, Col1a1, Rankl, Opg* and *Lcn-2* transcriptional levels were analyzed by real time-PCR.

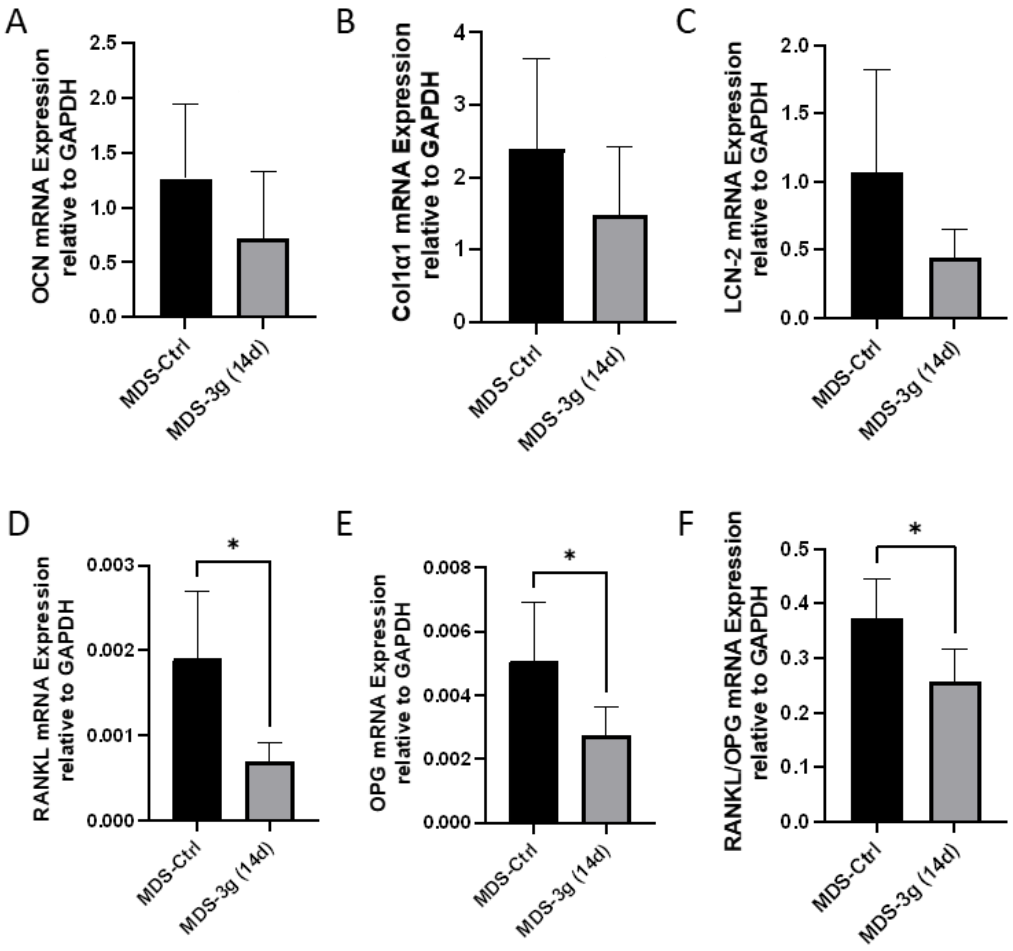

FIG. 22 GENE EXPRESSION OF EMPTY FEMUR OF MICE FROM 14-DAY 3G EXPOSURE. *OCN*: OSTEOCALCIN (A), *COL1A1*: COLLAGEN 1 ALPHA 1 (B), *LCN-2*: LIPOCALIN-2 (C), *RANKL*: RECEPTOR ACTIVATOR OF NUCLEAR FACTOR KAPPA-B LIGAND (D), *OPG*: OSTEOPROTEGERIN (E) AND *RANKL/OPG* (F). EXPERIMENT WAS PERFORMED AS ONE EXPERIMENT (N=6). DATA ARE SHOWN AS MEAN ± S.D, ONE-WAY ANOVA WITH WELCH CORRECTION, (*) P<0.05, (**) P<0.01, (***) P<0.001 E (****) P<0.0001.

It should be taken into consideration that the 14-day exposure to 3g was only a technical test with one MDS, and the initial number of animals was 6, which then decreased to 5 due to the removal of a mouse (as previously mentioned). A mild not significant reduction for *Ocn and Col1a1* (Fig-A-B) genes was observed after exposure to hypergravity, compared to control group. These results suggest that hypergravity stimulation for 14 days might lead to a reduction in bone differentiation or an impairment in bone homeostasis. Furthermore, given that *Lcn-2* is found upregulated in various microgravity conditions and that transgenic mice overexpressing *Lcn-2* exhibit osteopenia, we measured its mRNA levels (Fig 22-C) and observed a trend towards reduced expression in this condition, though it was not statistically significant. Both *Rankl* (Fig 22-D) and *Opg* (Fig 22-E)

exhibited decreased levels in hypergravity ($p \leqslant 0.05$ compared to control group). However, *Rankl/Opg* (Fig 22-F) ratio was also analyzed, in order to define which bone remodeling pathway was activated. *Rankl/Opg* ratio showed lower levels in MDS-3g compared to MDS-ctrl ($p \leqslant 0.05$ compared to control group), favoring bone deposition pathway.

3.2 TSP 2023: EFFECTS OF 27-DAYS EXPOSURE TO HYPERGRAVITY (3G)

After the pilot experiment carried out in 2019, a second experiment was conducted in 2023 with a larger number of mice, which were exposed to 3g for 27 days, in order to investigate the effects of a prolonged hypergravity exposure. We considered three groups: 12 mice from the vivarium (V) housed individually to reproduce the mice inside MDS condition, but in normal housing environment: regular cages dimensions, 20-22°C in the room, bedding and enrichment inside the cages; 12 mice housed individually (MDS-ctrl) in cages equal for dimension and material of the structure to MDS, 25°C as inside MDS, no bedding and enrichment to reproduce MDS environment; 11 mice housed individually (MDS-3g) in the payload MDS 25°C, no bedding and enrichment to ensure the cleaning of the cages by MDS subsystem during the experiment.

The acceleration of gravity was measured on the floor of the gondola showing a value of 3.2 g, while the g in the MDS cages experienced by the mice was maintained at 3 g. On the first day of the experiment, there was an acceleration ramp from 1 g to 3 g in 2 h. However, due to the reasons mentioned above (mice stopped drinking), on the second day, the acceleration was reduced to 2 g. Subsequently, the gravity level was brought back to 3 g on the following day, with no adverse effects observed in the mice.

Throughout the course of the experiment, there were several stops or reductions in the g value:

- On day 8, for water supply.
- On day 15 for water and food refurbishment
- On day 25 there was a reduction to 2 g due to a problem with the food supply which was then resolved remotely without requiring a total stop.
- On day 26 another stop to provide food to a cage (Cage 3 MDS module 2) and then returned after 2 hours to the value of 3 g.

These adjustments and interventions were made to ensure the well-being of the mice and the proper functioning of the experiment throughout its duration.

Similar to experiment conducted in 2019, temperatures and humidity of the 2 MDS modules, were monitored throughout all the experiment. Temperature and relative humidity are shown in Table 4.

TABLE 4 AVERAGE TEMPERATURE AND RELATIVE HUMIDITY ± SD INSIDE CAGES OF MDS 1 & 2

		Temperature (°C)	Relative humidity (%)
MDS 1	Cages 1-2-3	25.0±0.5	62.4±3.4
	Cages 4-5-6	24.8±0.5	54.4±1.3
MDS 2	Cages 1-2-3	24.6±1.4	45.7±1.8
	Cages 4-5-6	25.0±0.2	47.0±2.3

During the experiment, the temperature was stable and maintained similar values across all MDS cages. However, there were slight differences in relative humidity between the cages, particularly between cages 1-2-3 and 4-5-6 of MDS1 and between MDS 1 and MDS 2. It is important to note that despite these variations, all environmental parameters remained within a safe range for the animals, without creating secondary effects for the experiment. In the control cages (MDS-ctrl), the temperature was consistently around 25°C, and the relative humidity was maintained at 52% throughout the experiment.

Water consumption was monitored during the overall duration of the experiment. On the first day of the experiment, both cages exhibited water consumption of around 5 ml. However, with the increase in gravity acceleration at the beginning of the experiment on the LDC, there was a noticeable reduction in water consumption. In fact, the graphs indicate that water consumption dropped to zero on the second day (Fig.23).

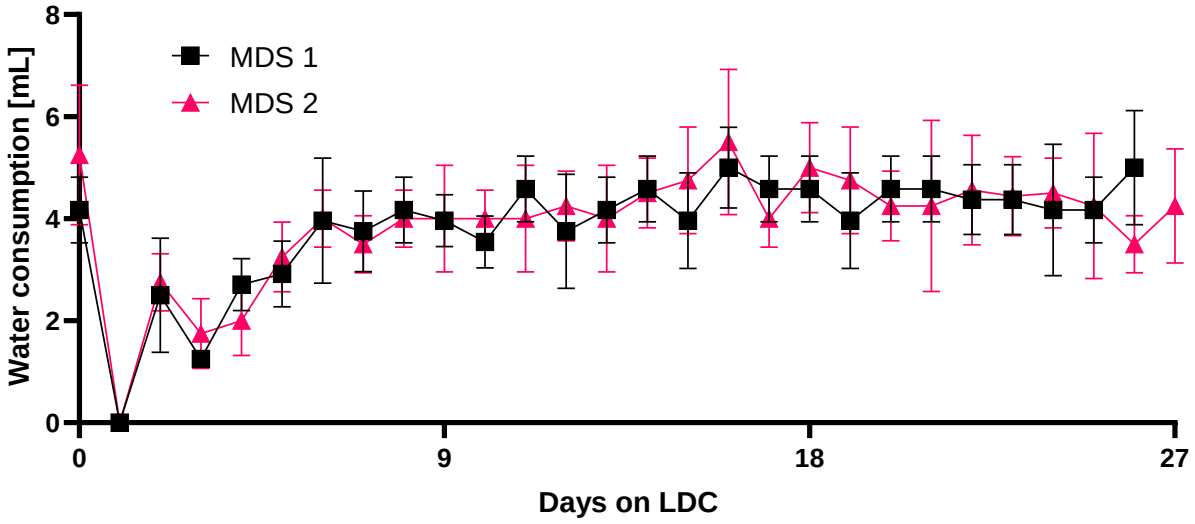

FIG. 23 WATER CONSUMPTION (ML) OF MICE FROM 3G EXPERIMENT DURING EACH DAY IN MDS 1 AND MDS 2. THE VALUES ARE EXPRESSED AS AVERAGE ± SD

For this reason, the acceleration was adjusted to 2G and maintained to this level for 1 day, to help the mice to adapt to this new condition. Subsequently, the graphs show that water consumption began to increase, signifying the recovery of the mice. Once again, the acceleration was increased to 3g, resulting in a decline in water consumption, which then started to increase until approximately 6 days after the start of the experiment and then stabilize until the end. As already mentioned, this effect was also documented in literature[88] and it was consistent with our previous findings from experiment conducted in 2019. Finally, in MDS-ctrl there were no large variations in daily water consumption.

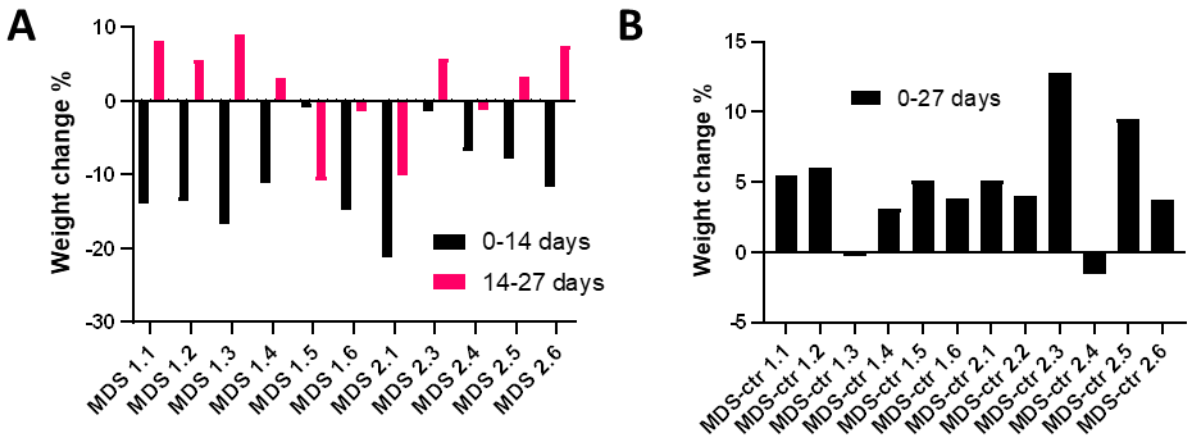

FIG. 24 WEIGHT CHANGE % OF MICE OF MDS-3G IN FIRST 2 WEEKS AND IN THE SECOND PART OF THE EXPERIMENT (A), OF MDS CTRL MICE IN ALL THE EXPERIMENT (B).

Mice were weighted at time 0, after 14 days (during the mandatory centrifuge stop) and after 27 days (at the end of the experiment before the TSP). Control mice inside the training cages showed a weight increase in almost all mice except 1.3 and 2.4. This increase may be related to the reduced number of possible movements of the animal inside the cage or the natural growth in weight of the animal (Fig.24-B). On the opposite side, mice exposed to hypergravity exhibited an initial average weight decrease of 10-20% during the first 2 weeks of the experiment. However, when looking at the second part of the experiment, there was an increase in weight, which indicated a partial recovery and therefore a possible adaptation to the hypergravity condition. This observed effect was consistent with findings from the 2019 experiment, confirming that hypergravity induced a weight decrease in mice initially, but this was followed by a recovery as they adapted to the hypergravity condition.

Further experiments will be needed to confirm that a prolonged exposure to hypergravity lead to a complete recovery of the mice.

3.2.1 Animal behaviour

Mice were monitored throughout the experiment, and the behavior was registered day by day with a dedicated video camera inside each cage.

Some observations were made during the whole experiment:

1st week: during the first week of exposure to hypergravity, all the mice fed on the food bars and started drinking from the third day of exposure. This behavior was a response to the stress induced by the increased acceleration, consistent with the findings from the previous experiment. Throughout the week, there were no issues with the mice's ability to eat or drink using the MDS system. The species-specific behavior of the mice was maintained, with some slight differences noted during this adaptation period. During the first 2 days of adaptation the mice explored the cage with reduced locomotor movements, performing behaviors similar to stretched postures, indicating a preference for resting behaviors. From the third day onward, the mice increased the frequency of maintenance behaviors (self-grooming, occasional face washing or scratching) and exploration behaviors (walking and rarely wall rearing). As expected, certain behaviors such as rearing, digging, or bar holding were almost totally suppressed during this first period of rotation.

2nd week: during the second week of hypergravity the mice fed and drank without any problems. Only some mice showed slightly different behaviors (feeding and drinking not every day). In particular, mouse 2.6 consumed less water while mice 1.4, 2.1 and 2.5 ate less in the last days of observation. From the behavioral point of view, the behaviors observed in the first week were mostly maintained. Vertical movements have been almost completely suppressed, with some rare events observed in this period. It is important to point out that the consumption of water and food requires the mouse to stand on its hind legs. The high frequency of these events highlights the possibility of these animals also being able to make vertical movements. During the first stop it was noticed that the animals tilted their heads slightly (not observed through the video). This tilting could be related to a potential imbalance in the otoliths between the two hemispheres.

3rd week: consumption by the mice remained normal during the third week and there was no change in species-specific behaviors. Regardless of the movements required for eating and drinking, vertical movements were rare.

4th week: During the fourth week the animals showed the same behaviors as the third both in feeding and in species-specific behaviors. After stopping the LDC and before the TSP the animals were studied inside a new cage for 5 minutes. The animals explored the cage and performed species-specific behaviors, with particular regard to locomotion, sniffing, and digging.

3.2.2 Blood analysis

Before euthanasia, blood samples were collected, under anesthesia, and classical blood parameters were analyzed to monitor animal general health. The number of red blood cells (RBC) showed a slight increase in MDS-ctrl mice compared to Vivarium (V) ($p \leqslant 0.05$) (Fig.26). The effect induced by hypergravity, when compared with MDS-CTRL, on RBC, HCT and HGB values and observed in the 2019 experiment was not detected in this 2023 experiment. This could be due to an adaptation of the animal after a longer exposure.

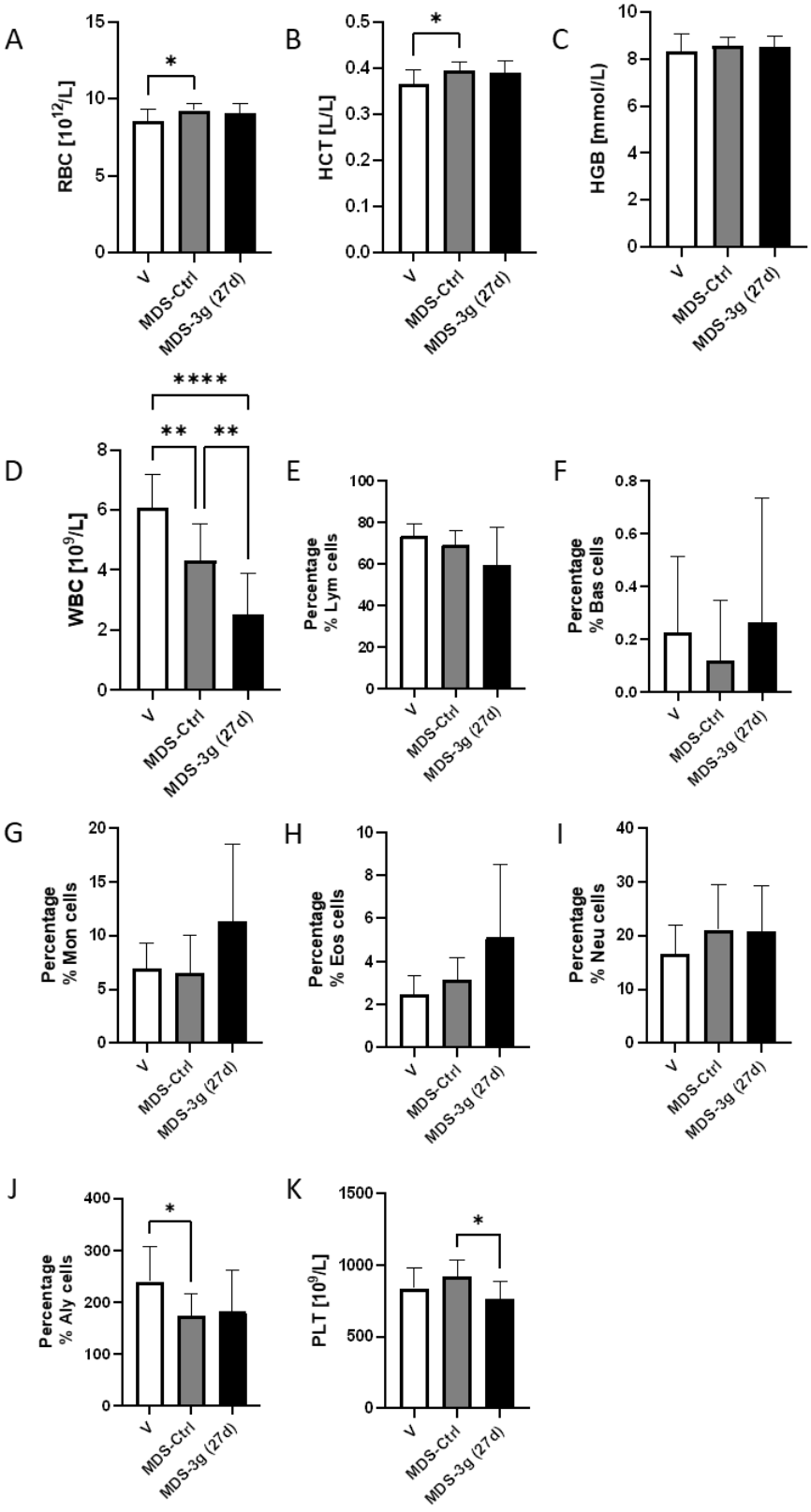

FIG. 25 BLOOD ANALYSYS OF MICE FROM 27 DAYS EXPERIMENT. DATA ARE SHOWN AS MEAN ± S.D, T- TEST WITH WELCH CORRECTION, (*) P<0.05, (**) P<0.01, (***) P<0.001. RBC: RED BLOOD CELLS (A), HCT: HEMATOCRIT (B), HGB:HEMOGLOBIN (C), WBC: WHITE BLOOD CELLS (D), LYM: LYMPHOCYTES (E), BAS:BASOPHIL (F), MON: MONOCYTES (G), EOS: EOSINOPHIL (H), NEU:NEUTROPHILS (I), ALY: ATYPICAL LYMPHOCYTES (J) AND PLT: PLATELET (K).

However, white blood cells (WBC) showed a decrease in MDS-ctrl compared to the Vivarium control group (Fig 25-D) ($p \leq 0.01$), and in MDS-3g compared to MDS-ctrl ($p \leq 0.01$). These data are in accordance to our previous findings observed in the 2019 TSP experiment, suggesting that the effect induced by hypergravity is maintained for the entire duration of the experiment, as also confirmed by Goldstein et al [89]. The same trend was found in the main lymphocyte population of WBC, although not statistically significant. No variations were found in percentage of basophils. Their increase is indeed generally correlated to infections[90]. Monocytes (Fig 25-G) exhibited a slight not statistically significant increase in MDS-3g compared to MDS-ctrl, in opposition to the strong increase displayed in the TSP-2019. Neutrophil (Fig 25-I) population displayed a slight not significant decrease in MDS-3g compared to MDS-ctrl. Finally, atypical lymphocytes showed a decrease in MDS-ctrl compared to Vivarium (Fig 25-J) ($p \leq 0.05$). The effect in this case could be attributed to the stress condition for the animal, as already described in the 14-day experiment above. Platelets enrichment was also investigated and no differences were observed between vivarium and MDS-ctrl, while a reduction in platelet number was detected in MDS-3g compared to MDS-ctrl (Fig 25-K) ($p \leq 0.05$), contrarily to what we observed in TSP-2019.

These findings confirm observations from the 2019 TSP experiment, indicating the persistence of a stress state in the animals during the experiment. This is evidenced by the analysis of the neutrophil-lymphocyte ratio as a biomarker of inflammation due to chronic stress: an increased variance in this ratio is present in the MDS-Ctrl group compared to the Vivarium ($p<0.05$)[86].

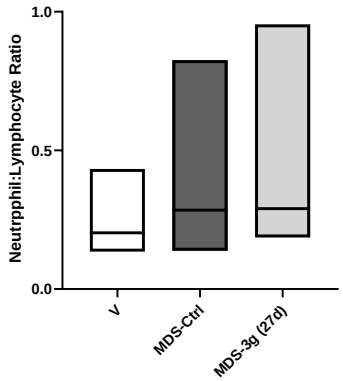

FIG. 26 NEUTROPHIL/LYMPHOCYTE RATIO OF MICE FROM 27 DAYS EXPERIMENT. DATA ARE SHOWN AS MEDIAN (LINE), MAX AND MIN VALUES (LIMITS OF EACH SQUARE) , T- TEST WITH WELCH CORRECTION ON VARIANCE RATIO, (*) P<0.05, (**) P<0.01, (***) P<0.001.

3.2.3 GENE EXPRESSION

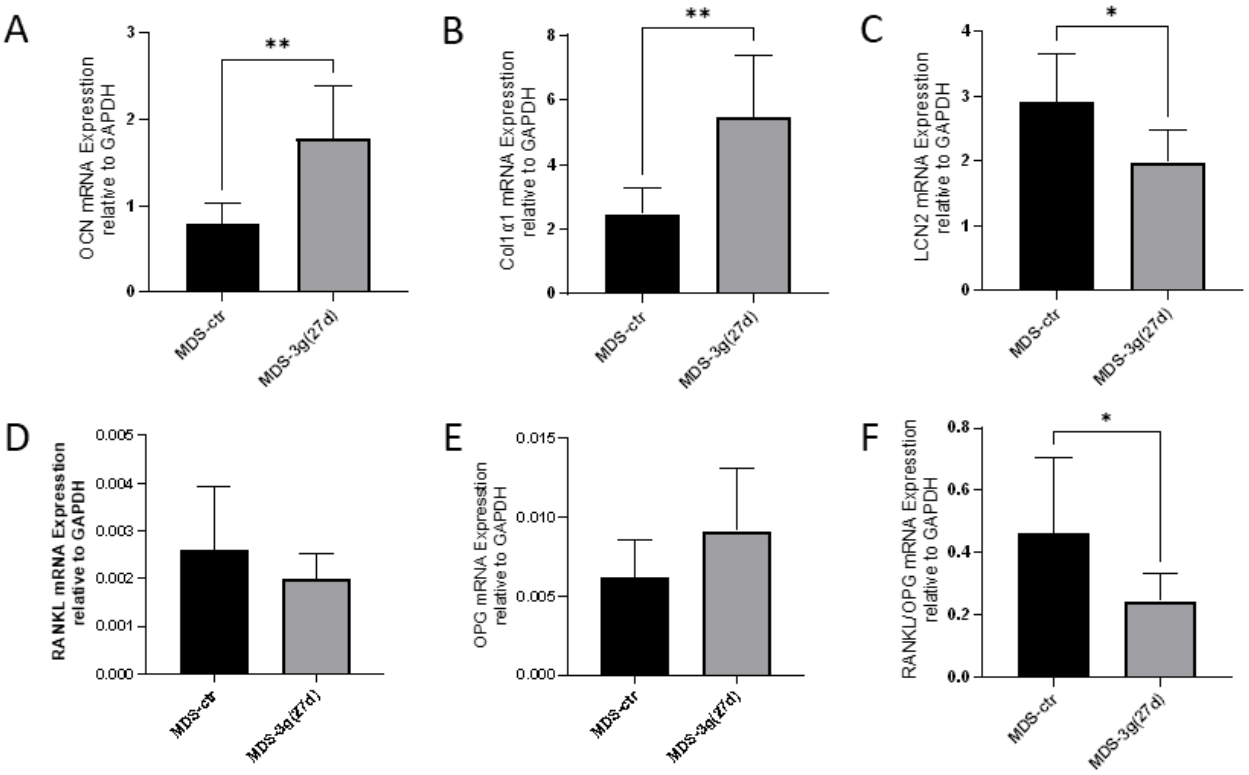

FIG. 27 GENE EXPRESSION OF EMPTY FEMUR OF MICE FROM 27 DAYS EXPERIMENT. *OCN*: OSTEOCALCIN (A), *COL1A1*: COLLAGEN 1 ALPHA 1 (B), *LCN-2*: LIPOCALIN-2 (C), *RANKL*: RECEPTOR ACTIVATOR OF NUCLEAR FACTOR KAPPA-B LIGAND (D), *OPG*: OSTEOPROTEGERIN (E) AND *RANKL/OPG* (F). EXPERIMENT WAS PERFORMED AS ONE EXPERIMENT (N=12). DATA ARE SHOWN AS MEAN ± S.D, ONE-WAY ANOVA WITH WELCH CORRECTION, (*) P<0.05, (**) P<0.01, (***) P<0.001 E (****) P<0.0001.

After euthanasia, femurs and tibiae were isolated, and RNA extraction was carried out from empty bones. Gene expression was evaluated to define the potential effects of hypergravity on the skeletal system. *Ocn, Col1a1*, *Lcn-2, Rankl and Opg* transcriptional levels were analyzed by real time-PCR.

Gene expression was carried on empty femurs, an increase in the expression of *Ocn* (Fig 27-A) ($p \leqslant 0.01$) and *Col1a1* (Fig 27-B) ($p \leqslant 0.01$) was found in mice exposed to hypergravity compared to control group.

Interestingly, *Lcn-2* mRNA (Fig 27-C) ($p \leqslant 0.05$) exhibited an opposite effect compared to our experiments of mice in simulated microgravity (HLU). *Lcn-2* seems to exert an effect dependent on the variation of gravitational force, suggesting that it has a role as a mechanoresponding protein, as also reported in literature[56,59,91,92].

These results could suggest that as far as the femur is loaded, we have an induction of bone formation, highlighted by an increase in genes correlated to bone formation (*Col1a1, Ocn*), and a decrease in genes related to bone resorption (Fig 27-D) (*Rankl*). This hypothesis was also confirmed by the increase of *Opg* (Fig 27-E) expression in MDS-3g compared to MDS-ctrl (even if not statistically significant) which, together with a decreased *Rankl/Opg* ratio (Fig 27-F) ($p \leq 0.05$), suggested that the favored pathway in 27-day 3g hypergravity experiment was bone formation.

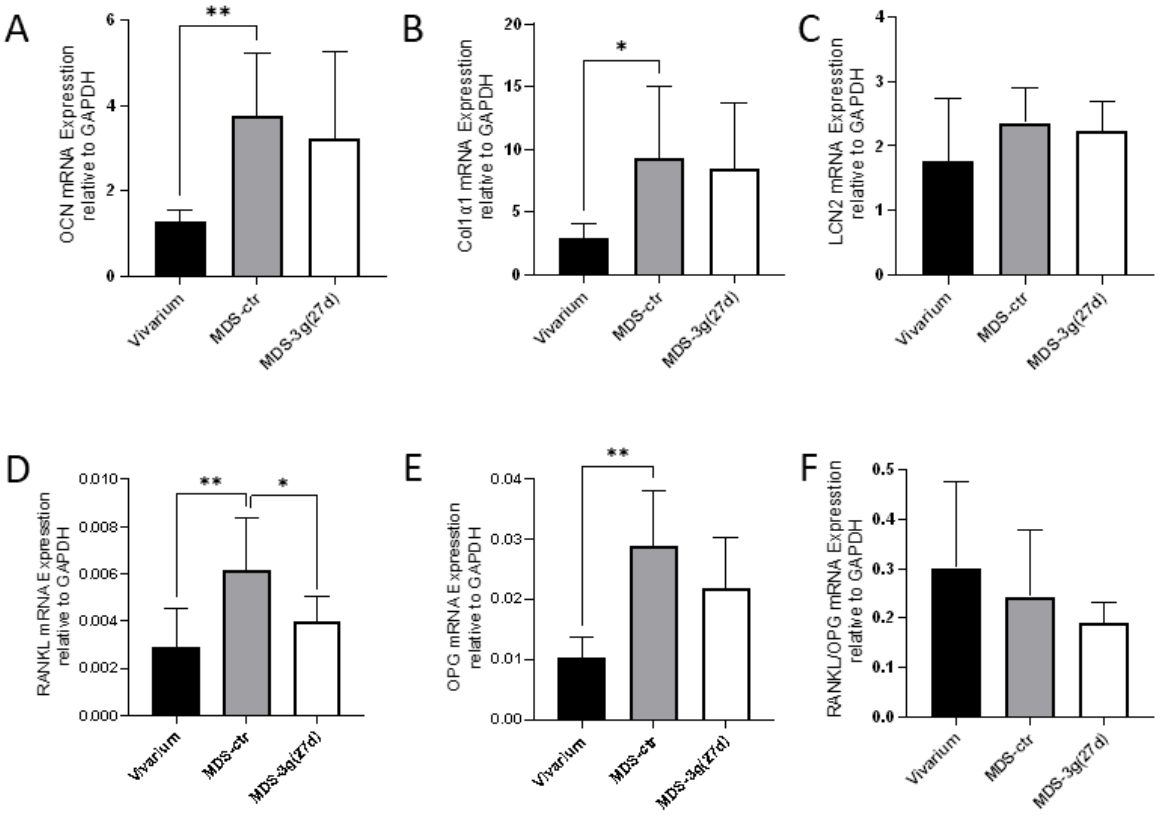

FIG. 28 GENE EXPRESSION OF EMPTY TIBIAE OF MICE FROM 27-DAY 3G. . *OCN*: OSTEOCALCIN (A), *COL1A1*: COLLAGEN 1 ALPHA 1 (B), *LCN-2*: LIPOCALIN-2 (C), *RANKL*: RECEPTOR ACTIVATOR OF NUCLEAR FACTOR KAPPA-B LIGAND (D), *OPG*: OSTEOPROTEGERIN (E) AND *RANKL/OPG* (F). EXPERIMENT WAS PERFORMED AS ONE EXPERIMENT (N=12). DATA ARE SHOWN AS MEAN ± S.D, ONE-WAY ANOVA WITH WELCH CORRECTION, (*) P<0.05, (**) P<0.01, (***) P<0.001 E (****) P<0.0001.

Gene expression on tibiae showed that, despite the smaller size of the cage, *Ocn* (Fig 28-A) ($p \leq 0.01$) and *Col1a1* (Fig 28-B) ($p \leq 0.05$) were upregulated in MDS-ctrl mice compared to V mice. We are currently analyzing the behavior of the mice in these two different conditions to determine if there was reduced movement in MDS-ctrl mice.

No significant variations in all genes between MDS-3g and MDS-ctrl except *Rankl* (Fig 28-D), which was found significantly downregulated in MDS-3g compared to MDS-ctrl ($p \leqslant 0.05$). On the contrary, no significant effects were observed on *Opg* expression, and also the *RANKL/OPG* ratio was not significantly different and only showed a slight decrease when comparing MDS-ctrl and MDS-3g. Notably, the only differing environmental parameter between the two conditions: MDS-ctrl and V, was the temperature, which was 20-22°C and 25°C respectively. On the other hand, an upregulation of *Rankl* (Fig 28-D) ($p \leqslant 0.01$), *Opg* (Fig 28-E) ($p \leqslant 0.01$), was observed in MDS-ctrl compared to Vivarium mice, while the *Rankl/Opg* (Fig 28-F) ratio remained unchanged suggesting that there was no significant increase in bone resorption in the tibia after 27 days of the 3g exposure.

3.2.4 MicroCT

MicroCT analysis was also carried out and preliminary results are reported on only 1 femur for each condition. The analysis of the other femurs is ongoing together with Inner ear, Calvaria and lumbar vertebra N°1-2. Classical histomorphometric parameters were considered: Bone volume (BV) represents the real volume that the bone has without considering the space inside (bone marrow) instead total volume (TV) is considering both components. The area analyzed are shown in Fig.29.

FIG. 29 FEMUR REGIONS ANALYZED BY MICRO CT

TABLE 5 BONE VOLUME (BV), TOTAL BONE VOLUME (TV) AND RATIO BV/TV OF THE DISTAL METAPHYSIS OF FEMUR.

	BV (µm³)	TV (µm³)	BV/TV (%)
V	1.30E+09	2.40E+10	5.4%
MDS-ctr	1.21E+09	2.40E+10	5.0%
MDS-3g	1.30E+09	2.40E+10	5.4%

TABLE 6 BONE VOLUME (BV), TOTAL BONE VOLUME (TV) ,RATIO BV/TV AND CORTICAL THICKNESS (C.TH) OF THE DIAPHYSIS OF FEMUR. DATA ARE EXPRESSED AS MEAN ± S.D (ONLY FOR C.TH).

	BV (µm³)	TV (µm³)	BV/TV (%)	C.Th (µm)
V	8.08E+08	1.44E+10	5.6%	27.29±8.00
MDS-ctr	9.52E+08	1.44E+10	6.6%	37.65±8.57
MDS-3g	9.75E+08	1.44E+10	6.8%	40.00±10.34

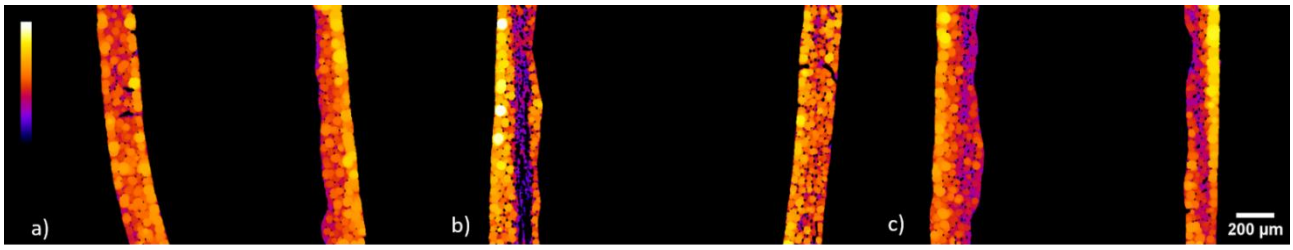

FIG. 30 COLOR MAP OF CORTICAL THICKNESS IN THE REGIONS OF THE FEMUR DIAPHYSIS. A) MDS-3G, B) VIVARIUM, C) MDS-CTRL

The data in Table 5 indicate that the distal metaphysis of MDS-ctrl displayed a slight decrease of BV/TV in MDS-ctrl compared to the V mouse. This value was rescued in MDS-3g mice after 27 days of exposure to 3g (Table 5). The cortical bone at the diaphysis showed a progressive increase of both BV/TV and C. Th. from V to MDS-ctrl to MDS-3g suggesting that hypergravity may have a positive effect on bones (Table 6). The color map highlights the greater thickness of the MDS-3g collar bone compared to the other two conditions (Fig. 30).

The data from the Vivarium comparing MDS-ctrl can be explained by what was obtained from the PCR of the femur and tibia where the effect of temperature had a significant reduction in bone metabolism and architecture.

4.0 DISCUSSION AND CONCLUSION

Since the first human spaceflight in 1961, the effects of space stress on the human body have been studied and reported in many ways. The first observation of microgravity-induced bone loss was recorded in the mid-1970s, when Skylab crew members demonstrated the loss of 1–2% bone mass per month compared to pre-flight and ground controls[93,94]. Since then, despite the implementation of preventative exercises, bone loss in space has been one of the most frequently observed outcomes among astronauts[95]. The weightlessness experienced in microgravity reduces the loading on weight-bearing bones, resulting in adaptive changes that increase bone resorption and inhibit bone formation[17]. Bone metabolism is indeed precisely maintained by the balance between osteoclastic bone resorption and new bone formation by osteoblasts[96] and mechanical force seems to play a critical role in regulating bone metabolism.

Despite the physiological relevance, relying solely on astronaut data to understand µ*g*-induced bone loss is limiting and rodent animal models (*in vivo*) such as HLU or cell models (*in vitro*) such as RPM have been developed to create conditions close to microgravity. Taking advantage from these models of simulated-µ*g*, several pathways have been recognized to contribute to bone loss in microgravity condition[97], such as Lipocalin-2 (LCN-2)[56,59]. LCN-2 is a pleiotropic protein, playing roles in cell proliferation, differentiation, and survival. However, its role in bone metabolism is poorly known. Some possible mechano-responding properties of LCN-2 have been already suggested. LCN-2 has been indeed recently reported as the most up-regulated gene in osteoblasts subjected to simulated microgravity, with an important negative effect on bone formation[98]. However, little is known on its precise role and mechanism in bone homeostasis impairment and osteopenia.

In this study we firstly analyzed the amount of LCN-2 in serum of tail-suspended in mice in HLU, observing an increase compared to control and confirming data already reported in literature. Furthermore, Rucci and colleagues also found a correlation between the exposure time in HLU and LCN-2 levels in the serum [56].

Different mechanisms have been proposed to be involved in triggering microgravity-related bone loss, including osteocytes apoptosis[19]. To elucidate the role of LCN-2 in bone metabolisms and to shed the light on activated pathways in osteocytes, we stimulated MLO-Y4 murine osteocytes with different concentrations of LCN-2 both in ground controls and in simulate microgravity. In both conditions, an upregulation of genes related to bone homeostasis was observed, such as *Cx43* and

E11. CX43 is a mechano-transducer protein [99–101] and its overexpression is in agreement with evidence reported in literature where a reduced amount of LCN-2 leads to a reduced expression of *Cx43* in PC-3 cells (carcinoma prostate cells with knockout of LCN-2)[102]. Interestingly, it has been showed that *CX43* overexpression aggravates apoptosis after cerebral ischemic injury[103]. Moreover, on the other hand, increased CX43 expression preserves osteocyte viability and maintain bone formation, preventing osteocytes apoptosis and preserving cortical bone quality[104]. According to all these findings many aspects remain to be elucidated and further experiments are essential to clarify the effect of LCN-2-induced overexpression of *Cx43*.

In addition, we also found that *Cx43* was upregulated in conditions of simulated-µ*g* (RPM). These data are in line with recent findings, showing a higher expression of this protein after 2h in RPM[105]. This effect was strengthened by the LCN-2 stimulation in microgravity, suggesting a synergic effect on bone impairment.

E11 is a protein involved in the formation and elongation of dendrites in osteocytes. Its upregulation after LCN-2 treatment suggests a role of LCN-2 in bone homeostasis. It is well known indeed that LCN-2 responds to reduced mechanical stimulation in bone and it is upregulated under mechanical unloading in mouse models as well as in humans[106]. On the other hand, *E11* expression was also found increased by a mechanical loading *in vivo* and maximal expression was observed in regions of potential bone remodelling, suggesting that dendrite elongation may be occurring during this process[62]. In parallel, *in vitro* studies demonstrated that MLO-Y4 cells show an increase in elongation of dendrites in response to shear stress, that is blocked by small interfering RNA specific to *E11* [62]. Furthermore, increased *E11* expression under mechanical stimuli might not be beneficial under certain conditions. Its overexpression in osteocytes was indeed observed in human and canine osteoarthritic subchondral bone[107]. Indeed, in osteoarthritic joints, the osteocytes in the subchondral bone exhibit alterations in their dendritic morphology, with fewer and more disorganised dendrites and *E11* overexpression seems to play a role in this impairment[107]. Therefore, LCN-2 induced *E11* overexpression observed in this study could confirm the role of LCN-2 in bone remodelling and alteration.

Expression of bone homeostasis-related genes, such as *Ppar-gamma*, *Sost* and *Ocn* was also evaluated after LCN-2 stimulation. PPAR-gamma is primarily an important marker of adipose tissue[64], but it was also described to have a role as negative regulator of bone formation by inhibiting

osteoblastogenesis from bone marrow cells[65]. In this study, *Ppar-gamma* was found strongly upregulated in LCN-2 stimulated osteocytes, suggesting that LCN-2 might induce bone remodeling and readaptation. As a confirmation, *Ppar-gamma* was downregulated in simulated microgravity, but LCN-2 stimulation in RPM was enough to determine again an increase in its expression. Furthermore, PPAR-GAMMA also has a role in the control of SOST expression as demonstrated by Baroi et al. In addition, PPAR-GAMMA increases osteoclast resorptive activities and commit BMSC toward adipocytes and away from osteoblasts, which partially explains PPAR-GAMMA negative effects on bone[108]. *Sost/Sclerostin* showed a comparable trend as *Ppar-gamma*. SOST has been reported as contributor in bone homeostasis, by regulating both osteoclastogenesis and osteoblast differentiation and activity[66,67]. In literature, it has been described that an overexpression of *SOST* in osteocytes might stimulate bone resorption[66]. According to our results, LCN-2 may act as an inducer of bone remodeling and resorption.

Finally, OCN was strongly downregulated in simulated microgravity, while LCN-2 treatment did not induce relevant effects on its expression, but only a mild increase. These results are in line with what reported by Deepak and colleagues, which described an increase of *Ocn*, parallel with an increase of mechanical loading on MLO-Y4 cells. On the other hand, an *Ocn* reduction was observed when these cells were subjected to simulated osteoporosis[109]. Furthermore, Yang et al found a downregulation of *Ocn* in MLO-Y4 cells after 6h of RPM[110]. This downregulation could be related to the characteristics of MLO-Y4 which could maintain borderline characteristics of osteoblasts and osteocytes. When osteoblasts are subjected to simulated microgravity they indeed exhibit a reduction in *Ocn*[111,112].

A pro-apoptotic effect of LCN-2 has been previously reported for different cell types. Xu et al. showed that LCN-2 treatment on cardiomyocytes led to the translocation of BAX to mitochondria, disruption of mitochondrial membrane potential and caspase-3 activation[113]. However, we did not observe an apoptotic effect after LCN-2 stimulation. We indeed highlighted an upregulation of both *Bax* and *Bcl-2,* which resulted in a null effect on their ratio. While BAX-BAX homodimers act as apoptosis inducers, BCL2-BAX heterodimer formation evokes indeed a survival signal for the cells.

Both *Bcl-2* and *Bax* are transcriptional targets for the tumor suppressor protein, P53, which induces cell cycle arrest or apoptosis in response to DNA damage[114] and it was upregulated by LCN-2 stimulation. Effect on *P53* expression are in line with previous studies on hematopoietic cells, in

which treatment with recombinant LCN-2 led to DNA damage, through intracellular ROS accumulation and P53 pathway activation[115]. In addition, expression of senescence-related genes *P21* and *P16* was also evaluated. The cyclin-dependent kinase inhibitor P21 is induced by both P53-dependent and -independent mechanisms following stress, and induction of P21 may cause cell cycle arrest. Cell cycle arrest permits cells to pause and to repair damage and then to continue cell division[116]. LCN-2 induces an increase in gene expression of *P21* in our hands, as well as an upregulation of *P16*. The *P16* gene belongs to INK4 family of genes, consisting of four members: P16 (INK4A), P15 (INK4B), P18 (INK4C) and P19 (INK4D). All the family members share biological properties, namely, inhibition of cell growth and tumor suppression. In our experiment P16 (like P53 and P21) was upregulated suggesting an induction to cell arrest and cell senescence.

On the other hand, simulated microgravity determined a downregulation of *Bax*, *Bcl-2* and *P53*. This downregulation is also reported in literature where exposure of human lymphocytes to simulated microgravity for 7 days led to a decrease of these genes [117]. RPM condition also downregulated *P16* gene. Pala and colleagues observed that simulated microgravity activate a molecular program of cell senescence, with an initial upregulation of senescence-related genes (i.e. *P53*, *P21*, *P16* and *P19*) after 6-12h, followed by a subsequent downregulation [118].

Taken together, these data suggest that LCN-2 stimulation may have a role in bone remodeling, determining an impairment in bone tissue with bone resorption preponderance. In addition, our data also demonstrated that LCN-2 does not have an apoptotic effect on osteocytes, but it may rather induce cellular senescence and cell cycle arrest in both ground control and simulated microgravity.

Furthermore, LCN-2 seems not to have an effect alone but it seems to have a synergic effect with simulated microgravity on the Bax/Bcl-2 ratio. Further tests need to be performed to confirm the biological effect.

In parallel to *in vitro* studies examining the role of microgravity and LCN-2 in bone cells, two experiments were conducted to determine whether hypergravity condition could mitigate the negative effects on the skeleton. Short-term and long-term effects of hypergravity on skeletal system were evaluated in two subsequent experiments, exposing mice to 3g gravitational force for 14 and 27 days, respectively. In both experiments, water consumption showed a drastic drop during

the first days of the experiment. Mice stopped drinking, due to their need to adapt to a new environment. This effect has been already described in literature by Dubayle and colleagues, which observed a reduction of water consumption in mice exposed to 2g gravitation force for 24 h[88].

We also observed a weight reduction of mice exposed to hypergravity. This can be attributed to two parallel causes, as supported by existing literature: hypergravity conditions can make it more challenging for mice to access and obtain food, and additionally, the combination of animal isolation, smaller size of the cage, absence of bedding and enrichment in the cages of MDS and hypergravity conditions can lead to increased stress levels in the animals[82,119]. This heightened stress response can negatively impact the mice's overall well-being and may contribute to weight loss. Interestingly, this effect was strongly detected in the short-term experiment and in the first two weeks of the long-term exposure, while mice started to gain weight after prolonged exposure, as already reported in literature [120–123].

Blood analyses also revealed interesting evidence. The increase in RBC was in opposition with observations in microgravity. Indeed, absence of the hydrostatic pressure in either simulated or true weightlessness causes a shift of blood to the head, an increase in circulation to the thorax and the head, and a subsequent reduction in total plasma volume (the so called 'Gauer-Henry reflex') through increased urine excretion. For instance, a decrease in RBC was observed in humans of the Skylab II, III and IV missions in the first phase of the mission (40 days). Interestingly, parameters were re-established at the initial values around the 100th day [124]. According to these findings, our data showed that RBC levels were restored to control levels in mice exposed to hypergravity for 27 days. On the other hand, our data also reported a decrease in WBC, according to recent findings from Goldstein et al, showing a decrease in WBC from 7 days till the end of the experiment (30 days) when mice were exposed to 1.6 g[89]. Monocytes fluctuations were investigated in microgravity experiments. The effect of microgravity on monocyte numbers appears to be effective only during the end of the experiment. Kaur et al saw a statistically significant increase in the number of monocytes in astronauts immediately after the mission, compared to before the launch, while no variation was observed during the microgravity condition. Perhaps a rapid, but brief increase in monocytes may result from launch or upon initial exposure to spaceflight, but the effect is transient and dissipates after a few days of spaceflight[125]. According to these reporting, our long-term experiment also showed that after 27 days of exposure to hypergravity, monocytes levels in mice are restored to control levels. The transient increase observed in astronauts could be related to the

deceleration during re-entry into the atmosphere similar to what occurs in mice exposed to 3 g (in normal orbital launch and re-entry missions an astronaut is subjected on average to 3 g of acceleration/deceleration[126]). Furthermore, Farahani et al observed an increase in eosinophils upon the return of astronauts from space, as happens with monocytes, and this could be due either to the exposure to microgravity or to the brief exposure to hypergravity upon re-entry into the atmosphere[127]. On the other side, Goldstein et al [89] previously reported a sharp decline of neutrophil after 6 days, which returns to the original values at day 7. This is presumably due to the stress of the new environment.

Finally, also an increase in platelets was observed after short-term exposure to hypergravity (14 days), while a decrease was registered after long-term exposure (27 days). Dai and colleagues already described a reduced haemostasis on mice after exposure in simulated microgravity (HLU), also confirmed *in vitro* by a reduced number of adherent platelets (3h in Rotary Cell Culture System (RCCS)). In hypergravity, contrarily, they observed an increase in haemostasis and a high number of adherent platelets, confirming what we observed[128]. In addition, it has been described that hypergravity stimulation for a short period (i.e., three days) led to an increase in the number of platelets in mice when compared to control conditions. However, this effect appeared to reach a peak on day 10 and subsequently declined on day 21, confirming our data of transient increase in platelets blood enrichment[129].

Taken together, our data on blood parameters confirmed that hypergravity seems to be detrimental for mice in the first period of hypergravity exposure, but this is due to the mice adaptation to the new environment. Mice vital parameters are indeed restored to normal levels after long-term exposure, as they adapted to the cages and to the high gravitational force.

Finally, gene expression reported that hypergravity may induce bone deposition, based on our results on *Rankl/Opg* ratio. In microgravity it has been demonstrated that this ratio is higher, thus favoring bone resorption[130–132]. Our findings on femur of mice exposed for 27 days to hypergravity revealed that the ratio is lower compared to the control favoring bone deposition. This relationship was also demonstrated by Kawao et al, where stimulation of mice at 3g for 4 weeks led to a reduction in the *Rankl/Opg* ratio [40].

We also reported a downregulation of both *Col1a1* and *Ocn* after short-term exposure to hypergravity, an opposite and statistical significant effect was detectable after 27 days of exposition, confirming the previous results suggesting a predominance of bone deposition.

Interestingly, we found a higher expression of bone markers in MDS-ctrl compared to Vivarium mice. Although, normally the cages in the vivarium are larger than those for MDS-ctrl, allowing mice more space to move, Vivarium mice were kept at a lower temperature for almost 48 weeks of experiment compared to MDS-ctrl and MDS-3g (~20°C instead of 25°C). The combined effect of low temperature and isolated housing conditions might have had an effect on energy expenditure and bone homeostasis. This observation are in line with unpublished data from personal communication with Laurence Vico.

The preliminary results from MicroCT suggest that hypergravity can induce bone formation and stop bone resorption. These data confirm what was seen in our previous work, where the exposure of 4 mice for 90 days to 2g led to an increase in BV/TV and C.Th of control mice [44]. These data will be complemented by further analyzes that are ongoing.

Finally, our study has shown that a 27-day exposure to 3g, hypergravity decreases LCN-2 mRNA expression in the femur, coinciding with enhanced expression of bone formation markers such as collagen type I and osteocalcin, along with a lowered *Rankl/Opg* mRNA ratio, suggesting a reduction in bone resorption.

These findings confirm the crucial role of LCN-2 within the mechanobiology of bone across different gravitational environments and underscore the need for further research into hypergravity's capacity to modulate bone density and integrity.

5.0 BIBLIOGRAPHY

(1) Rodan, G. A. Introduction to Bone Biology. *Bone* **1992**, *13*, S3–S6. https://doi.org/10.1016/S8756-3282(09)80003-3.

(2) Srivastava, R. K.; Sapra, L.; Mishra, P. K. Osteometabolism: Metabolic Alterations in Bone Pathologies. *Cells* **2022**, *11* (23). https://doi.org/10.3390/CELLS11233943.

(3) Bonewald, L. F. The Amazing Osteocyte. *J. Bone Miner. Res.* **2011**, *26* (2), 229–238. https://doi.org/10.1002/JBMR.320.

(4) Datta, H. K.; Ng, W. F.; Walker, J. A.; Tuck, S. P.; Varanasi, S. S. The Cell Biology of Bone Metabolism. *J. Clin. Pathol.* **2008**, *61* (5), 577–587. https://doi.org/10.1136/JCP.2007.048868.

(5) Oftadeh, R.; Perez-Viloria, M.; Villa-Camacho, J. C.; Vaziri, A.; Nazarian, A. Biomechanics and Mechanobiology of Trabecular Bone: A Review. *J. Biomech. Eng.* **2015**, *137* (1). https://doi.org/10.1115/1.4029176.

(6) Buck, D. W.; Dumanian, G. A. Bone Biology and Physiology: Part I. The Fundamentals. *Plast. Reconstr. Surg.* **2012**, *129* (6), 1314–1320. https://doi.org/10.1097/PRS.0B013E31824ECA94.

(7) Newton's Law of Universal Gravitation - Wikipedia.

(8) Fournier, R.; Harrison, R. E. Strategies for Studying Bone Loss in Microgravity. *REACH* **2020**, *17–20*. https://doi.org/10.1016/J.REACH.2020.100036.

(9) *Extended Stays in Space | NASA*. https://www.nasa.gov/1ym/about (accessed 2021-01-24).

(10) Julius von Sachs - Digital Collections - National Library of Medicine.

(11) Clinostats @ Userweb.Ucs.Louisiana.Edu.

(12) Borst, A. G.; Van Loon, J. J. W. A. Technology and Developments for the Random Positioning Machine, RPM. *Microgravity Sci. Technol.* **2009**, *21* (4), 287–292. https://doi.org/10.1007/s12217-008-9043-2.

(13) Bae, Y. H.; Park, K.; Mrsny, R. J. *Cancer Targeted Drug Delivery: An Elusive Dream*; 2013; Vol.

9781461478. https://doi.org/10.1007/978-1-4614-7876-8.

(14) Man, J.; Graham, T.; Squires-Donelly, G.; Laslett, A. L. The Effects of Microgravity on Bone Structure and Function. *NPJ Microgravity* **2022**, *8* (1). https://doi.org/10.1038/S41526-022-00194-8.

(15) Vico, L.; Collet, P.; Guignandon, A.; Lafage-Proust, M. H.; Thomas, T.; Rehailia, M.; Alexandre, C. Effects of Long-Term Microgravity Exposure on Cancellous and Cortical Weight-Bearing Bones of Cosmonauts. *Lancet* **2000**, *355* (9215), 1607–1611. https://doi.org/10.1016/S0140-6736(00)02217-0.

(16) Kenkre, J. S.; Bassett, J. H. D. The Bone Remodelling Cycle. *Ann. Clin. Biochem.* **2018**, *55* (3), 308–327. https://doi.org/10.1177/0004563218759371.

(17) Caillot-Augusseau, A.; Lafage-Proust, M. H.; Soler, C.; Pernod, J.; Dubois, F.; Alexandre, C. Bone Formation and Resorption Biological Markers in Cosmonauts during and after a 180-Day Space Flight (Euromir 95). *Clin. Chem.* **1998**, *44* (3), 578–585. https://doi.org/10.1093/CLINCHEM/44.3.578.

(18) Rodionova, N. V; Oganov, V. S.; Zolotova, N. V. Ultrastructural Changes in Osteocytes in Microgravity Conditions. *Adv. Space Res.* **2002**, *30* (4), 765–770. https://doi.org/10.1016/S0273-1177(02)00393-9.

(19) Gerbaix, M.; Gnyubkin, V.; Farlay, D.; Olivier, C.; Ammann, P.; Courbon, G.; Laroche, N.; Genthial, R.; Follet, H.; Peyrin, F.; Shenkman, B.; Gauquelin-Koch, G.; Vico, L. One-Month Spaceflight Compromises the Bone Microstructure, Tissue-Level Mechanical Properties, Osteocyte Survival and Lacunae Volume in Mature Mice Skeletons. *Sci. Reports 2017 71* **2017**, *7* (1), 1–12. https://doi.org/10.1038/s41598-017-03014-2.

(20) Aguirre, J. I.; Plotkin, L. I.; Stewart, S. A.; Weinstein, R. S.; Parfitt, A. M.; Manolagas, S. C.; Bellido, T. Osteocyte Apoptosis Is Induced by Weightlessness in Mice and Precedes Osteoclast Recruitment and Bone Loss. *J. Bone Miner. Res.* **2006**, *21* (4), 605–615. https://doi.org/10.1359/JBMR.060107.

(21) Sundblad, P.; Orlov, O.; Angerer, O.; Larina, I.; Cromwell, R. Standardization of Bed Rest

Studies in the Spaceflight Context. *J. Appl. Physiol.* **2016**, *121* (1), 348–349. https://doi.org/10.1152/JAPPLPHYSIOL.00089.2016.

(22) Lloyd, S. A.; Lewis, G. S.; Zhang, Y.; Paul, E. M.; Donahue, H. J. Connexin 43 Deficiency Attenuates Loss of Trabecular Bone and Prevents Suppression of Cortical Bone Formation during Unloading. *J. Bone Miner. Res.* **2012**, *27* (11), 2359–2372. https://doi.org/10.1002/JBMR.1687.

(23) Lewiecki, E. M. Role of Sclerostin in Bone and Cartilage and Its Potential as a Therapeutic Target in Bone Diseases. *Ther. Adv. Musculoskelet. Dis.* **2014**, *6* (2), 48–57. https://doi.org/10.1177/1759720X13510479.

(24) Smith, S. M.; Heer, M.; Shackelford, L. C.; Sibonga, J. D.; Spatz, J.; Pietrzyk, R. A.; Hudson, E. K.; Zwart, S. R. Bone Metabolism and Renal Stone Risk during International Space Station Missions. *Bone* **2015**, *81*, 712–720. https://doi.org/10.1016/J.BONE.2015.10.002.

(25) Spatz, J. M.; Fields, E. E.; Yu, E. W.; Divieti Pajevic, P.; Bouxsein, M. L.; Sibonga, J. D.; Zwart, S. R.; Smith, S. M. Serum Sclerostin Increases in Healthy Adult Men during Bed Rest. *J. Clin. Endocrinol. Metab.* **2012**, *97* (9), E1736–E1740. https://doi.org/10.1210/JC.2012-1579.

(26) Lacey, D. L.; Timms, E.; Tan, H. L.; Kelley, M. J.; Dunstan, C. R.; Burgess, T.; Elliott, R.; Colombero, A.; Elliott, G.; Scully, S.; Hsu, H.; Sullivan, J.; Hawkins, N.; Davy, E.; Capparelli, C.; Eli, A.; Qian, Y. X.; Kaufman, S.; Sarosi, I.; Shalhoub, V.; Senaldi, G.; Guo, J.; Delaney, J.; Boyle, W. J. Osteoprotegerin Ligand Is a Cytokine That Regulates Osteoclast Differentiation and Activation. *Cell* **1998**, *93* (2), 165–176. https://doi.org/10.1016/S0092-8674(00)81569-X.

(27) Boyle, W. J.; Simonet, W. S.; Lacey, D. L. Osteoclast Differentiation and Activation. *Nat. 2003 4236937* **2003**, *423* (6937), 337–342. https://doi.org/10.1038/nature01658.

(28) Yu, W.; Zhong, L.; Yao, L.; Wei, Y.; Gui, T.; Li, Z.; Kim, H.; Holdreith, N.; Jiang, X.; Tong, W.; Dyment, N.; Sherry Liu, X.; Yang, S.; Choi, Y.; Ahn, J.; Qin, L. Bone Marrow Adipogenic Lineage Precursors Promote Osteoclastogenesis in Bone Remodeling and Pathologic Bone Loss. *J. Clin. Invest.* **2021**, *131* (2). https://doi.org/10.1172/JCI140214.

(29) Hughes-Fulford, M. Function of the Cytoskeleton in Gravisensing during Spaceflight. *Adv.*

Space Res. **2003**, *32* (8), 1585–1593. https://doi.org/10.1016/S0273-1177(03)90399-1.

(30) Guignandon, A.; Usson, Y.; Laroche, N.; Lafage-Proust, M. H.; Sabido, O.; Alexandre, C.; Vico, L. Effects of Intermittent or Continuous Gravitational Stresses on Cell-Matrix Adhesion: Quantitative Analysis of Focal Contacts in Osteoblastic ROS 17/2.8 Cells. *Exp. Cell Res.* **1997**, *236* (1), 66–75. https://doi.org/10.1006/EXCR.1997.3703.

(31) Dai, Z. Q.; Wang, R.; Ling, S. K.; Wan, Y. M.; Li, Y. H. Simulated Microgravity Inhibits the Proliferation and Osteogenesis of Rat Bone Marrow Mesenchymal Stem Cells. *Cell Prolif.* **2007**, *40* (5), 671–684. https://doi.org/10.1111/J.1365-2184.2007.00461.X.

(32) Nabavi, N.; Khandani, A.; Camirand, A.; Harrison, R. E. Effects of Microgravity on Osteoclast Bone Resorption and Osteoblast Cytoskeletal Organization and Adhesion. *Bone* **2011**, *49* (5), 965–974. https://doi.org/10.1016/J.BONE.2011.07.036.

(33) Tamma, R.; Colaianni, G.; Camerino, C.; Benedetto, A. Di; Greco, G.; Strippoli, M.; Vergari, R.; Grano, A.; Mancini, L.; Mori, G.; Colucci, S.; Grano, M.; Zallone, A. Microgravity during Spaceflight Directly Affects in Vitro Osteoclastogenesis and Bone Resorption. *FASEB J.* **2009**, *23* (8), 2549–2554. https://doi.org/10.1096/FJ.08-127951.

(34) Cabahug-Zuckerman, P.; Frikha-Benayed, D.; Majeska, R. J.; Tuthill, A.; Yakar, S.; Judex, S.; Schaffler, M. B. Osteocyte Apoptosis Caused by Hindlimb Unloading Is Required to Trigger Osteocyte RANKL Production and Subsequent Resorption of Cortical and Trabecular Bone in Mice Femurs. *J. Bone Miner. Res.* **2016**, *31* (7), 1356–1365. https://doi.org/10.1002/JBMR.2807.

(35) Blaber, E. A.; Dvorochkin, N.; Lee, C.; Alwood, J. S.; Yousuf, R.; Pianetta, P.; Globus, R. K.; Burns, B. P.; Almeida, E. A. C. Microgravity Induces Pelvic Bone Loss through Osteoclastic Activity, Osteocytic Osteolysis, and Osteoblastic Cell Cycle Inhibition by CDKN1a/P21. *PLoS One* **2013**, *8* (4), e61372. https://doi.org/10.1371/JOURNAL.PONE.0061372.

(36) V. On the Direction of the Radicle and Germen during the Vegetation of Seeds. By Thomas Andrew Knight, Esq. F. R. S. In a Letter to the Right Hon. Sir Joseph Banks, K. B. P. R. S. *Philos. Trans. R. Soc. London* **1806**, *96*, 99–108. https://doi.org/10.1098/RSTL.1806.0006.

(37) Young, L. R. Artificial Gravity Considerations for a Mars Exploration Mission. *Ann. N. Y. Acad. Sci.* **1999**, *871*, 367–378. https://doi.org/10.1111/J.1749-6632.1999.TB09198.X.

(38) Ciofani, G.; Ricotti, L.; Rigosa, J.; Menciassi, A.; Mattoli, V.; Monici, M. Hypergravity Effects on Myoblast Proliferation and Differentiation. *J. Biosci. Bioeng.* **2012**, *113* (2), 258–261. https://doi.org/10.1016/J.JBIOSC.2011.09.025.

(39) Woodcock, E. M.; Girvan, P.; Eckert, J.; Lopez-Duarte, I.; Eta Kubánková, M.; Van Loon, J. J. W. A.; Brooks, N. J.; Kuimova, M. K. Measuring Intracellular Viscosity in Conditions of Hypergravity. **2019**. https://doi.org/10.1016/j.bpj.2019.03.038.

(40) Kawao, N.; Morita, H.; Obata, K.; Tamura, Y.; Okumoto, K.; Kaji, H. The Vestibular System Is Critical for the Changes in Muscle and Bone Induced by Hypergravity in Mice. *Physiol. Rep.* **2016**, *4* (19). https://doi.org/10.14814/PHY2.12979.

(41) Stock, J. T. Wolff's Law (Bone Functional Adaptation). *Int. Encycl. Biol. Anthropol.* **2018**, 1–2. https://doi.org/10.1002/9781118584538.IEBA0521.

(42) Vico, L.; Barou, O.; Laroche, N.; Alexandre, C.; Lafage-Proust, M. H. Effects of Centrifuging at 2g on Rat Long Bone Metaphyses. *Eur. J. Appl. Physiol. Occup. Physiol.* **1999**, *80* (4), 360–366. https://doi.org/10.1007/S004210050604/METRICS.

(43) Tominari, T.; Ichimaru, R.; Taniguchi, K.; Yumoto, A.; Shirakawa, M.; Matsumoto, C.; Watanabe, K.; Hirata, M.; Itoh, Y.; Shiba, D.; Miyaura, C.; Inada, M. Hypergravity and Microgravity Exhibited Reversal Effects on the Bone and Muscle Mass in Mice. *Sci. Rep.* **2019**, *9* (1). https://doi.org/10.1038/S41598-019-42829-Z.

(44) Canciani, B.; Ruggiu, A.; Giuliani, A.; Panetta, D.; Marozzi, K.; Tripodi, M.; Salvadori, P. A.; Cilli, M.; Ohira, Y.; Cancedda, R.; Tavella, S. Effects of Long Time Exposure to Simulated Micro- and Hypergravity on Skeletal Architecture. *J. Mech. Behav. Biomed. Mater.* **2015**, *51*, 1–12. https://doi.org/10.1016/J.JMBBM.2015.06.014.

(45) *ESA - ESA centrifuge*. https://www.esa.int/ESA_Multimedia/Images/2018/01/ESA_centrifuge (accessed 2023-10-01).

(46) Donovan, F.; Espinosa, P. D. G. P. S. P.; Boyle, P. M. R.; Scientist, G. C. Potential NASA Rodent Centrifuge Artificial Gravity Workshop. **2016**.

(47) Large Diameter Centrifuge (LDC) Experimenter Users Manual. **2019**.

(48) *STS-128 - NASA*. https://www.nasa.gov/mission/sts-128/ (accessed 2023-10-01).

(49) *STS-129 - NASA*. https://www.nasa.gov/mission/sts-129/ (accessed 2023-10-01).

(50) Cancedda, R.; Liu, Y.; Ruggiu, A.; Tavella, S.; Biticchi, R.; Santucci, D.; Schwartz, S.; Ciparelli, P.; Falcetti, G.; Tenconi, C.; Cotronei, V.; Pignataro, S. The Mice Drawer System (MDS) Experiment and the Space Endurance Record-Breaking Mice. *PLoS One* **2012**, *7* (5), e32243. https://doi.org/10.1371/JOURNAL.PONE.0032243.

(51) Bishop, R. E.; Cambillau, C.; Privé, G. G.; Hsi, D.; Tillo, D.; Tillier, E. R. M. Bacterial Lipocalins: Origin, Structure, and Function. **2013**.

(52) Campanacci, V.; Nurizzo, D.; Spinelli, S.; Valencia, C.; Tegoni, M.; Cambillau, C. The Crystal Structure of the Escherichia Coli Lipocalin Blc Suggests a Possible Role in Phospholipid Binding. *FEBS Lett.* **2004**, *562* (1–3), 183–188. https://doi.org/10.1016/S0014-5793(04)00199-1.

(53) Flower, D. R.; North, A. C. T.; Attwood, T. K. In the Lipocalins and Related Proteins. *Protein Sci.* **1993**, 753–761.

(54) Capulli, M.; Ponzetti, M.; Maurizi, A.; Gemini-Piperni, S.; Berger, T.; Mak, T. W.; Teti, A.; Rucci, N. A Complex Role for Lipocalin 2 in Bone Metabolism: Global Ablation in Mice Induces Osteopenia Caused by an Altered Energy Metabolism. *J. Bone Miner. Res.* **2018**, *33* (6), 1141–1153. https://doi.org/10.1002/jbmr.3406.

(55) Costa, D.; Principi, E.; Lazzarini, E.; Descalzi, F.; Cancedda, R.; Castagnola, P.; Tavella, S. LCN2 Overexpression in Bone Enhances the Hematopoietic Compartment via Modulation of the Bone Marrow Microenvironment. *J. Cell. Physiol.* **2017**, *232* (11), 3077–3087. https://doi.org/10.1002/jcp.25755.

(56) Rucci, N.; Capulli, M.; Piperni, S. G.; Cappariello, A.; Lau, P.; Frings-Meuthen, P.; Heer, M.; Teti,

A. Lipocalin 2: A New Mechanoresponding Gene Regulating Bone Homeostasis. *J. Bone Miner. Res.* **2015**, *30* (2), 357–368. https://doi.org/10.1002/jbmr.2341.

(57) Rosser, J.; Bonewald, L. F. Studying Osteocyte Function Using the Cell Lines MLO-Y4 and MLO-A5. *Methods Mol. Biol.* **2012**, *816*, 67–81. https://doi.org/10.1007/978-1-61779-415-5_6.

(58) Morey-Holton, E. R.; Globus, R. K. Hindlimb Unloading Rodent Model: Technical Aspects. *J. Appl. Physiol.* **2002**, *92* (4), 1367–1377. https://doi.org/10.1152/JAPPLPHYSIOL.00969.2001/ASSET/IMAGES/LARGE/DG0421440005.JPEG.

(59) Veeriah, V.; Zanniti, A.; Paone, R.; Chatterjee, S.; Rucci, N.; Teti, A.; Capulli, M. Interleukin-1β, Lipocalin 2 and Nitric Oxide Synthase 2 Are Mechano-Responsive Mediators of Mouse and Human Endothelial Cell-Osteoblast Crosstalk. *Sci. Rep.* **2016**, *6*. https://doi.org/10.1038/SREP29880.

(60) Basso, N.; Heersche, J. N. M. Effects of Hind Limb Unloading and Reloading on Nitric Oxide Synthase Expression and Apoptosis of Osteocytes and Chondrocytes. *Bone* **2006**, *39* (4), 807–814. https://doi.org/10.1016/J.BONE.2006.04.014.

(61) Xu, H.; Gu, S.; Riquelme, M. A.; Burra, S.; Callaway, D.; Cheng, H.; Guda, T.; Schmitz, J.; Fajardo, R. J.; Werner, S. L.; Zhao, H.; Shang, P.; Johnson, M. L.; Bonewald, L. F.; Jiang, J. X. Connexin 43 Channels Are Essential for Normal Bone Structure and Osteocyte Viability. *J. Bone Miner. Res.* **2015**, *30* (3), 550. https://doi.org/10.1002/JBMR.2374.

(62) Zhang, K.; Barragan-Adjemian, C.; Ye, L.; Kotha, S.; Dallas, M.; Lu, Y.; Zhao, S.; Harris, M.; Harris, S. E.; Feng, J. Q.; Bonewald, L. F. E11/Gp38 Selective Expression in Osteocytes: Regulation by Mechanical Strain and Role in Dendrite Elongation. *Mol. Cell. Biol.* **2006**, *26* (12), 4539. https://doi.org/10.1128/MCB.02120-05.

(63) Hau, C. S.; Kanda, N.; Tada, Y.; Shibata, S.; Uozaki, H.; Fukusato, T.; Sato, S.; Watanabe, S. Lipocalin-2 Exacerbates Psoriasiform Skin Inflammation by Augmenting T-Helper 17 Response. *J. Dermatol.* **2016**, *43* (7), 785–794. https://doi.org/10.1111/1346-8138.13227.

(64) Cipolletta, D.; Feuerer, M.; Li, A.; Kamei, N.; Lee, J.; Shoelson, S. E.; Benoist, C.; Mathis, D.

PPAR-γ Is a Major Driver of the Accumulation and Phenotype of Adipose Tissue Treg Cells. *Nat. 2012 4867404* **2012**, *486* (7404), 549–553. https://doi.org/10.1038/nature11132.

(65) Marie, P. J.; Kaabeche, K. PPAR Gamma Activity and Control of Bone Mass in Skeletal Unloading. *PPAR Res.* **2006**. https://doi.org/10.1155/PPAR/2006/64807.

(66) Delgado-Calle, J.; Sato, A. Y.; Bellido, T. Role and Mechanism of Action of Sclerostin in Bone. *Bone* **2017**, *96*, 29. https://doi.org/10.1016/J.BONE.2016.10.007.

(67) Bellido, T. Osteocyte-Driven Bone Remodeling. *Calcif. Tissue Int.* **2014**, *94* (1), 25–34. https://doi.org/10.1007/S00223-013-9774-Y.

(68) Capulli, M.; Paone, R.; Rucci, N. Osteoblast and Osteocyte: Games without Frontiers. *Arch. Biochem. Biophys.* **2014**, *561*, 3–12. https://doi.org/10.1016/J.ABB.2014.05.003.

(69) Dewson, G.; Kluck, R. M. Mechanisms by Which Bak and Bax Permeabilise Mitochondria during Apoptosis. *J. Cell Sci.* **2009**, *122* (16), 2801. https://doi.org/10.1242/JCS.038166.

(70) Korsmeyer, S. J.; Shutter, J. R.; Veis, D. J.; Merry, D. E.; Oltvai, Z. N. Bcl-2/Bax: A Rheostat That Regulates an Anti-Oxidant Pathway and Cell Death. *Semin. Cancer Biol.* **1993**, *4* (6), 327–332.

(71) Marie Hardwick, J.; Soane, L. Multiple Functions of BCL-2 Family Proteins. *Cold Spring Harb. Perspect. Biol.* **2013**, *5* (2). https://doi.org/10.1101/CSHPERSPECT.A008722.

(72) Vaskivuo, T. E.; Stenbäck, F.; Tapanainen, J. S. Apoptosis and Apoptosis-Related Factors Bcl-2, Bax, Tumor Necrosis Factor-α, and NF-KB in Human Endometrial Hyperplasia and Carcinoma. *Cancer* **2002**, *95* (7), 1463–1471. https://doi.org/10.1002/CNCR.10876.

(73) Shaw, P. H. The Role of P53 in Cell Cycle Regulation. *Pathol. - Res. Pract.* **1996**, *192* (7), 669–675. https://doi.org/10.1016/S0344-0338(96)80088-4.

(74) Leblanc, A.; Schneider, V.; Shackelford, L.; West, S.; Oganov, V.; Bakulin, A.; Voronin, L. Bone Mineral and Lean Tissue Loss after Long Duration Space Flight. *J Musculoskel Neuron Interact* **2000**, *1* (2), 157–160.

(75) Vico, L.; van Rietbergen, B.; Vilayphiou, N.; Linossier, M. T.; Locrelle, H.; Normand, M.; Zouch,

M.; Gerbaix, M.; Bonnet, N.; Novikov, V.; Thomas, T.; Vassilieva, G. Cortical and Trabecular Bone Microstructure Did Not Recover at Weight-Bearing Skeletal Sites and Progressively Deteriorated at Non-Weight-Bearing Sites During the Year Following International Space Station Missions. *J. Bone Miner. Res.* **2017**, *32* (10), 2010–2021. https://doi.org/10.1002/JBMR.3188.

(76) Costa, D.; Lazzarini, E.; Canciani, B.; Giuliani, A.; Spanò, R.; Marozzi, K.; Manescu, A.; Cancedda, R.; Tavella, S. Altered Bone Development and Turnover in Transgenic Mice Over-Expressing Lipocalin-2 in Bone. *J. Cell. Physiol.* **2013**, *228* (11), 2210–2221. https://doi.org/10.1002/JCP.24391.

(77) Michaletti, A.; Gioia, M.; Tarantino, U.; Zolla, L. Effects of Microgravity on Osteoblast Mitochondria: A Proteomic and Metabolomics Profile. *Sci. Rep.* **2017**, *7* (1). https://doi.org/10.1038/S41598-017-15612-1.

(78) Nguyen, H. P.; Tran, P. H.; Kim, K. S.; Yang, S. G. The Effects of Real and Simulated Microgravity on Cellular Mitochondrial Function. *NPJ microgravity* **2021**, *7* (1). https://doi.org/10.1038/S41526-021-00171-7.

(79) Iandolo, D.; Strigini, M.; Guignandon, A.; Vico, L. Osteocytes and Weightlessness. *Curr. Osteoporos. Rep.* **2021**, *19* (6), 626–636. https://doi.org/10.1007/S11914-021-00713-8.

(80) Du, J.; Yang, J.; He, Z.; Cui, J.; Yang, Y.; Xu, M.; Qu, X.; Zhao, N.; Yan, M.; Li, H.; Yu, Z. Osteoblast and Osteoclast Activity Affect Bone Remodeling Upon Regulation by Mechanical Loading-Induced Leukemia Inhibitory Factor Expression in Osteocytes. *Front. Mol. Biosci.* **2020**, *7*, 585056. https://doi.org/10.3389/FMOLB.2020.585056/BIBTEX.

(81) Picquet, F.; Dupont, E.; Cochon, L.; Montel, V.; Bojados, M.; Jamon, M.; Bastide, B.; Stevens, L.; Picquet, F.; Dupont, E.; Cochon, L.; Montel, V.; Bojados, M.; Jamon, M.; Bastide, B.; Stevens, L. Adaption of Mice Muscle Properties in Hypo/Hypergravity Environment. *ESASP* **2013**, *706* (1), 40.

(82) Guéguinou, N.; Bojados, M.; Jamon, M.; Derradji, H.; Baatout, S.; Tschirhart, E.; Frippiat, J. P.; Legrand-Frossi, C. Stress Response and Humoral Immune System Alterations Related to Chronic Hypergravity in Mice. *Psychoneuroendocrinology* **2012**, *37* (1), 137–147.

https://doi.org/10.1016/J.PSYNEUEN.2011.05.015.

(83) Bojados, M.; Jamon, M. The Long-Term Consequences of the Exposure to Increasing Gravity Levels on the Muscular, Vestibular and Cognitive Functions in Adult Mice. *Behav. Brain Res.* **2014**, *264*, 64–73. https://doi.org/10.1016/J.BBR.2014.01.018.

(84) Gnyubkin, V.; Guignandon, A.; Laroche, N.; Vanden-Bossche, A.; Normand, M.; Lafage-Proust, M. H.; Vico, L. Effects of Chronic Hypergravity: From Adaptive to Deleterious Responses in Growing Mouse Skeleton. *J. Appl. Physiol.* **2015**, *119* (8), 908–917. https://doi.org/10.1152/JAPPLPHYSIOL.00364.2015.

(85) Research, N. R. C. (US) I. for L. A. Guide for the Care and Use of Laboratory Animals. *Guid. Care Use Lab. Anim.* **1996**. https://doi.org/10.17226/5140.

(86) McDonald, L. T.; Lopez, M. F.; Helke, K. L.; McCrackin, M. A.; Cray, J. J.; Becker, H. C.; LaRue, A. C. Early Blood Profile of C57BL/6 Mice Exposed to Chronic Unpredictable Stress. *Front. Psychiatry* **2019**, *10* (APR), 448791. https://doi.org/10.3389/FPSYT.2019.00230/BIBTEX.

(87) Sampson, A. P. The Role of Eosinophils and Neutrophils in Inflammation. *Clin. Exp. Allergy* **2000**, *30* (1), 22–27. https://doi.org/10.1046/J.1365-2222.2000.00092.X.

(88) Dubayle, D.; Vanden-Bossche, A.; Peixoto, T.; Morel, J. L. Hypergravity Increases Blood–Brain Barrier Permeability to Fluorescent Dextran and Antisense Oligonucleotide in Mice. *Cells* **2023**, *12* (5), 734. https://doi.org/10.3390/CELLS12050734/S1.

(89) Goldstein, O.; Ishay, J. S. The White Blood Cell Line: Changes Induced in Mice by Hypergravity. *Adv. Sp. Res.* **1998**, *21* (8–9), 1333–1343. https://doi.org/10.1016/S0273-1177(97)00654-6.

(90) Borriello, F.; Granata, F.; Marone, G. Basophils and Skin Disorders. *J. Invest. Dermatol.* **2014**, *134* (5), 1202–1210. https://doi.org/10.1038/JID.2014.16.

(91) Veeriah, V.; Paone, R.; Chatterjee, S.; Teti, A.; Capulli, M. Osteoblasts Regulate Angiogenesis in Response to Mechanical Unloading. *Calcif. Tissue Int.* **2019**, *104* (3), 344–354. https://doi.org/10.1007/S00223-018-0496-Z/METRICS.

(92) Veeriah, V.; Capulli, M.; Zanniti, A.; Chatterjee, S.; Rucci, N.; Teti, A. The Critical Biomechanical

Role of Lipocalin 2 in the Crosstalk between Endothelium and Osteoblasts in Unloading Conditions. *Bone Abstr.* **2016**, *5*. https://doi.org/10.1530/BONEABS.5.OC6.3.

(93) Collet, P.; Uebelhart, D.; Vico, L.; Moro, L.; Hartmann, D.; Roth, M.; Alexandre, C. Effects of 1- and 6-Month Spaceflight on Bone Mass and Biochemistry in Two Humans. *Bone* **1997**, *20* (6), 547–551. https://doi.org/10.1016/S8756-3282(97)00052-5.

(94) Rambaut, P. C.; Johnston, R. S. Prolonged Weightlessness and Calcium Loss in Man. *Acta Astronaut.* **1979**, *6* (9), 1113–1122. https://doi.org/10.1016/0094-5765(79)90059-6.

(95) Sibonga, J. D.; Evans, H. J.; Sung, H. G.; Spector, E. R.; Lang, T. F.; Oganov, V. S.; Bakulin, A. V.; Shackelford, L. C.; LeBlanc, A. D. Recovery of Spaceflight-Induced Bone Loss: Bone Mineral Density after Long-Duration Missions as Fitted with an Exponential Function. *Bone* **2007**, *41* (6), 973–978. https://doi.org/10.1016/J.BONE.2007.08.022.

(96) Martin, T. J.; Gooi, J. H.; Sims, N. A. Molecular Mechanisms in Coupling of Bone Formation to Resorption. *Crit. Rev. Eukaryot. Gene Expr.* **2009**, *19* (1), 73–88. https://doi.org/10.1615/CRITREVEUKARGENEEXPR.V19.I1.40.

(97) Zhang, P.; Hamamura, K.; Yokota, H. A Brief Review of Bone Adaptation to Unloading. *Genomics. Proteomics Bioinformatics* **2008**, *6* (1), 4–7. https://doi.org/10.1016/S1672-0229(08)60016-9.

(98) Capulli, M.; Rufo, A.; Teti, A.; Rucci, N. Global Transcriptome Analysis in Mouse Calvarial Osteoblasts Highlights Sets of Genes Regulated by Modeled Microgravity and Identifies a "Mechanoresponsive Osteoblast Gene Signature." *J. Cell. Biochem.* **2009**, *107* (2), 240–252. https://doi.org/10.1002/JCB.22120.

(99) Costa, E.; Thrasivoulou, C.; Becker, D. L.; Deprest, J. A.; David, A. L.; Chowdhury, T. T.; Thrasivoulou, C.; Deprest, J.; Becker, D.; David, A.; Chowdhury, T. Cx43 Regulates Mechanotransduction Mechanisms in Human Preterm Amniotic Membrane Defects. *Prenat. Diagn.* **2023**, *43* (10), 1284–1295. https://doi.org/10.1002/PD.6429.

(100) Cherian, P. P.; Siller-Jackson, A. J.; Gu, S.; Wang, X.; Bonewald, L. F.; Sprague, E.; Jiang, J. X. Mechanical Strain Opens Connexin 43 Hemichannels in Osteocytes: A Novel Mechanism for

the Release of Prostaglandin. *Mol. Biol. Cell* **2005**, *16* (7), 3100–3106. https://doi.org/10.1091/MBC.E04-10-0912/ASSET/IMAGES/LARGE/ZMK0070571970006.JPEG.

(101) Riquelme, M. A.; Cardenas, E. R.; Xu, H.; Jiang, J. X. The Role of Connexin Channels in the Response of Mechanical Loading and Unloading of Bone. *Int. J. Mol. Sci. 2020, Vol. 21, Page 1146* **2020**, *21* (3), 1146. https://doi.org/10.3390/IJMS21031146.

(102) Schröder, S. K.; Pinoé-Schmidt, M.; Weiskirchen, R. Lipocalin-2 (LCN2) Deficiency Leads to Cellular Changes in Highly Metastatic Human Prostate Cancer Cell Line PC-3. *Cells* **2022**, *11* (2). https://doi.org/10.3390/CELLS11020260.

(103) Chen, B.; Yang, L.; Chen, J.; Chen, Y.; Zhang, L.; Wang, L.; Li, X.; Li, Y.; Yu, H. Inhibition of Connexin43 Hemichannels with Gap19 Protects Cerebral Ischemia/Reperfusion Injury via the JAK2/STAT3 Pathway in Mice. *Brain Res. Bull.* **2019**, *146*, 124–135. https://doi.org/10.1016/J.BRAINRESBULL.2018.12.009.

(104) Davis, H. M.; Aref, M. W.; Aguilar-Perez, A.; Pacheco-Costa, R.; Allen, K.; Valdez, S.; Herrera, C.; Atkinson, E. G.; Mohammad, A.; Lopez, D.; Harris, M. A.; Harris, S. E.; Allen, M.; Bellido, T.; Plotkin, L. I. Cx43 Overexpression in Osteocytes Prevents Osteocyte Apoptosis and Preserves Cortical Bone Quality in Aging Mice. *JBMR Plus* **2018**, *2* (4), 206. https://doi.org/10.1002/JBM4.10035.

(105) Xu, H.; Liu, R.; Ning, D.; Zhang, J.; Yang, R.; Riquelme, M. A.; Li, J.; Jiang, J. X.; Shang, P. Biological Responses of Osteocytic Connexin 43 Hemichannels to Simulated Microgravity. *J. Orthop. Res.* **2017**, *35* (6), 1195–1202. https://doi.org/10.1002/JOR.23224.

(106) Maurizi, A.; Ponzetti, M.; Gautvik, K. M.; Reppe, S.; Teti, A.; Rucci, N. Lipocalin 2 Serum Levels Correlate with Age and Bone Turnover Biomarkers in Healthy Subjects but Not in Postmenopausal Osteoporotic Women. *Bone Reports* **2021**, *14*, 101059. https://doi.org/10.1016/J.BONR.2021.101059.

(107) Staines, K. A.; Ikpegbu, E.; Törnqvist, A. E.; Dillon, S.; Javaheri, B.; Amin, A. K.; Clements, D. N.; Buttle, D. J.; Pitsillides, A. A.; Farquharson, C. Conditional Deletion of E11/Podoplanin in Bone Protects against Load-Induced Osteoarthritis. *BMC Musculoskelet. Disord.* **2019**, *20* (1), 1–11.

https://doi.org/10.1186/S12891-019-2731-9/FIGURES/6.

(108) Baroi, S.; Czernik, P. J.; Chougule, A.; Griffin, P. R.; Lecka-Czernik, B. PPARG in Osteocytes Controls Sclerostin Expression, Bone Mass, Marrow Adiposity and Mediates TZD-Induced Bone Loss. *Bone* **2021**, *147*, 115913. https://doi.org/10.1016/J.BONE.2021.115913.

(109) Deepak, V.; Kayastha, P.; McNamara, L. M. Estrogen Deficiency Attenuates Fluid Flow-Induced [Ca2+]i Oscillations and Mechanoresponsiveness of MLO-Y4 Osteocytes. *FASEB J.* **2017**, *31* (7), 3027–3039. https://doi.org/10.1096/FJ.201601280R.

(110) Yang, X.; Sun, L. W.; Wu, X. T.; Wang, X. N.; Fan, Y. B. Effect of Simulated Microgravity on Osteocytes Responding to Fluid Shear Stress. *Acta Astronaut.* **2013**, *84*, 237–243. https://doi.org/10.1016/J.ACTAASTRO.2012.10.018.

(111) Carmeliet, G.; Nys, G.; Stockmans, I.; Bouillon, R. Gene Expression Related to the Differentiation of Osteoblastic Cells Is Altered by Microgravity. *Bone* **1998**, *22* (5), 139S-143S. https://doi.org/10.1016/S8756-3282(98)00007-6.

(112) Ontiveros, C.; McCabe, L. R. Simulated Microgravity Suppresses Osteoblast Phenotype, Runx2 Levels and AP-1 Transactivation. *J. Cell. Biochem.* **2003**, *88* (3), 427–437. https://doi.org/10.1002/JCB.10410.

(113) Xu, G.; Ahn, J. H.; Chang, S. Y.; Eguchi, M.; Ogier, A.; Han, S. J.; Park, Y. S.; Shim, C. Y.; Jang, Y. S.; Yang, B.; Xu, A.; Wang, Y.; Sweeney, G. Lipocalin-2 Induces Cardiomyocyte Apoptosis by Increasing Intracellular Iron Accumulation. *J. Biol. Chem.* **2012**, *287* (7), 4808–4817. https://doi.org/10.1074/JBC.M111.275719.

(114) Basu, A.; Haldar, S. The Relationship between BcI2, Bax and P53: Consequences for Cell Cycle Progression and Cell Death. *Mol. Hum. Reprod.* **1998**, *4* (12), 1099–1109. https://doi.org/10.1093/MOLEHR/4.12.1099.

(115) Kagoya, Y.; Yoshimi, A.; Tsuruta-Kishino, T.; Arai, S.; Satoh, T.; Akira, S.; Kurokawa, M. JAK2V617F+ Myeloproliferative Neoplasm Clones Evoke Paracrine DNA Damage to Adjacent Normal Cells through Secretion of Lipocalin-2. *Blood* **2014**, *124* (19), 2996–3006. https://doi.org/10.1182/BLOOD-2014-04-570572.

(116) *The Role of the Cyclin-dependent Kinase Inhibitor p21 in Apoptosis 1 | Molecular Cancer Therapeutics | American Association for Cancer Research*. https://aacrjournals.org/mct/article/1/8/639/233906/The-Role-of-the-Cyclin-dependent-Kinase-Inhibitor (accessed 2023-10-15).

(117) Fukazawa, T.; Tanimoto, K.; Shrestha, L.; Imura, T.; Takahashi, S.; Sueda, T.; Hirohashi, N.; Hiyama, E.; Yuge, L. Simulated Microgravity Enhances CDDP-Induced Apoptosis Signal via P53-Independent Mechanisms in Cancer Cells. *PLoS One* **2019**, *14* (7), e0219363. https://doi.org/10.1371/JOURNAL.PONE.0219363.

(118) Pala, R.; Cruciani, S.; Manca, A.; Garroni, G.; EL Faqir, M. A.; Lentini, V.; Capobianco, G.; Pantaleo, A.; Maioli, M. Mesenchymal Stem Cell Behavior under Microgravity: From Stress Response to a Premature Senescence. *Int. J. Mol. Sci. 2023, Vol. 24, Page 7753* **2023**, *24* (9), 7753. https://doi.org/10.3390/IJMS24097753.

(119) Yuwaki, K.; Okuno, M. Changes in Food Intake and Growth Rate in Mice under Hypergravity. *Biol. Sci. Space.* **2003**.

(120) Wade, C. E.; Harper, J. S.; Daunton, N. G.; Corcoran, M. L.; Morey-Holton, E. Body Mass Change during Altered Gravity: Spaceflight, Centrifugation, and Return to 1 G. *J. Gravit. Physiol.* **1997**, *4* (3), 43–48.

(121) Thorling, E. B.; Fredens, K. The Influence of Small Changes in the Gravitational Field on the Weight Regulation in Female Wistar Rats. *Int. J. Obes.* **1995**, *19* (5), 305–309.

(122) Pitts, G. C.; Bull, L. S.; Oyama, J. Regulation of Body Mass in Rats Exposed to Chronic Acceleration. *https://doi.org/10.1152/ajplegacy.1975.228.3.714* **1975**, *228* (3), 714–717. https://doi.org/10.1152/AJPLEGACY.1975.228.3.714.

(123) Kita, S.; Shibata, S.; Kim, H.; Otsubo, A.; Ito, M.; Iwasaki, K. Dose-Dependent Effects of Hypergravity on Body Mass in Mature Rats.

(124) Economos, A. C. REGULATION OF HAEMOPOIESIS IN ALTERED GRAVITY. *Biol. Rev.* **1981**, *56* (2), 87–98. https://doi.org/10.1111/J.1469-185X.1981.TB00344.X.

(125) Kaur, I.; Simons, E. R.; Castro, V. A.; Ott, C. M.; Pierson, D. L. Changes in Monocyte Functions of Astronauts. *Brain. Behav. Immun.* **2005**, *19* (6), 547–554. https://doi.org/10.1016/J.BBI.2004.12.006.

(126) Jackson, E. An Investigation of the Effects of Sustained G-Forces on the Human Body During Suborbital Spaceflight Master of Science in Aerospace Engineering. **2017**.

(127) Mostofizadeh Farahani, R.; DiPietro Farahani RM, L. A.; Microgravity and, D. LA. Microgravity and the Implications for Wound Healing. *Int. Wound J.* **2008**, *5* (4), 552–561. https://doi.org/10.1111/J.1742-481X.2008.00438.X.

(128) Dai, K.; Wang, Y.; Yan, R.; Shi, Q.; Wang, Z.; Yuan, Y.; Cheng, H.; Li, S.; Fan, Y.; Zhuang, F. Effects of Microgravity and Hypergravity on Platelet Functions. *Thromb. Haemost.* **2009**, *101* (5), 902–910. https://doi.org/10.1160/TH08-11-0750/ID/JR0750-7/BIB.

(129) Pecaut, M. J.; Miller, G. M.; Nelson, G. A.; Gridley, D. S. Hypergravity-Induced Immunomodulation in a Rodent Model: Hematological and Lymphocyte Function Analyses. *J. Appl. Physiol.* **2004**, *97* (1), 29–38. https://doi.org/10.1152/JAPPLPHYSIOL.01304.2003/ASSET/IMAGES/LARGE/ZDG0070431520005.JPEG.

(130) Rucci, N.; Rufo, A.; Alamanou, M.; Teti, A. Modeled Microgravity Stimulates Osteoclastogenesis and Bone Resorption by Increasing Osteoblast RANKL/OPG Ratio. *J. Cell. Biochem.* **2007**, *100* (2), 464–473. https://doi.org/10.1002/JCB.21059.

(131) Chatziravdeli, V.; Katsaras, G. N.; Lambrou, G. I. Gene Expression in Osteoblasts and Osteoclasts Under Microgravity Conditions: A Systematic Review. *Curr. Genomics* **2019**, *20* (3), 184–198. https://doi.org/10.2174/1389202920666190422142053.

(132) Rucci, N.; Capulli, M.; Rufo, A.; Teti, A. The Effect of Microgravity on Osteoblast Metabolism. **2009**, *19* (3), 139–149.